

5 FORMULATION & DEVELOPMENT OF DRUG AND GENE DUAL LOADED PLHNCS

5.1 INTRODUCTION

Polymer lipid hybrid nanocarriers are a mixture of the properties of liposomes and nanoparticles that have a beneficial size range (10-200 nm) desirable for endocytic intercellular uptake, aggregation by leaky tumor vascular structures at the tumor site, which is useful for sustained tumor site drug exposure and good structural stability (1). One technique includes a two-step procedure in which the polymer core and lipid shell are separately prepared and then inserted and blended together and the other technique involves a single-step process in which the hybrid nanoparticles are prepared using a single-step system of nanoprecipitation and self-assembly. The viability of all the methods described in Chapter 2 was tested and the best approach appropriate for the preparation of Docetaxel PLHNCS with favourable features was further optimized. The particle size and encapsulation efficiency were selected as quality target profile. Plackett-Burman design (PBD) and Box-Behnken design (BBD) was employed as the second statistical design to fully elucidate the formulation development parameters. Further, the optimized PLHNCS formulation was subjected to lyophilization using various cryoprotectants to increase drug retention and dry powder inhaler was developed using different grade of modified lactose to achieve better aerodynamic properties.

5.2 MATERIALS AND INSTRUMENTS

5.2.1 Materials

Table 5-1 List of materials used with their sources

Sr no.	Material Category	Name	Supplier of Material
1	Drug	Docetaxel	Gift sample from Sun Pharmaceuticals Advanced Research Center (SPARC)
2	Gene	ABCB1 shRNA plasmid	SCBT, USA
2	Polymer	PLGA (50:50)	Gift Sample from PURAC England
		PLGA (75:25)	
		PEG: Polycaprolactone (PEG: PCL)	Sigma Aldrich

		PEG: Poly lactic acid (PEG: PLA)	Sigma Aldrich
3	Phospholipids	Phospholipoin 90G (Soy Phosphatidylcholine)	Gift samples from Lipoid, Germany
		Egg Phosphatidylcholine	
		1,2-dipalmitoyl-sn-glycero-3-phosphocholine (DPPC)	
		Cholesterol	
		Didioleoyl trimethylammoniumpropane (DOTAP)	
		Dioleoyl phosphatidyl ethanolamine (DOPE)	
		1,2-distearoyl-sn-glycero-3-phosphoethanolamine-N-[carboxy(polyethylene glycol)-2000] (sodium salt) (DSPE-PEG)	
4	Solvents	Acetone (analytical grade)	S D Fine Chemicals, India
		Chloroform (analytical grade)	
		Potassium Dihydrogen Phosphate	
		Sodium hydroxide Pellets	
		Glacial Acetic acid	
		Hydrochloric Acid	S.D. Fine Chemicals
		Sodium Acetate Trihydrate	Lipoid GmbH, Germany.
		Acetonitrile (analytical grade)	Thermo fisher scientific, USA
		Acetonitrile (HPLC grade)	Thermo fisher scientific, USA

5.2.2 Equipments

Table 5-2 List of Equipments Used

Sr. No.	Equipment	Company
1.	Single pan electronic balance	Type AX 120 & ELB 300, Shimadzu
2.	UV Visible Spectrophotometer	UV-1800, Shimadzu, Japan
3.	HPLC	Agilent Technologies 1260 infinity II
4.	Bath sonicator	Sartorius, India
5.	Probe sonicator	Sartorius AG, Germany.
6.	Magnetic stirrer	Remi, India
7.	Virtis Advantage Plus Lyophilizer	Virtis
8.	Centrifuge (CPR-30)	Remi Elektrotechnik Ltd., Mumbai, India

9.	Dialysis Membrane-70 (pore size 7000 daltons, Diameter 27.3 mm)	Himedia Laboratories Pvt. Ltd. Mumbai.
10	Extruder	Avestin, USA
11	BioSpec-nanodrop 1000	BioRad Lab., USA
12	Malvern Zetasizer Nano ZS	Malvern Instruments, Malvern, UK
13	Transmission Electron Microscopy	TECNAI G2 Spirit BioT WIN, FEI-Netherlands

5.3 FORMULATION AND DEVELOPMENT

5.3.1 Method of preparation

Formulations of PLHNCs were performed using modified single-step nano-precipitation method which involves self-assembly of polymers and various ratios of lipids (2). Two phases (i.e., organic and aqueous) were prepared separately and then, mixed together to form PLHNCs. A fixed quantity of PEG: PCL (1-10 mg/mL) and Docetaxel were dissolved in acetonitrile to prepare the organic phase. DPPC: DOTAP: DSPE-PEG₂₀₀₀ was dissolved in 4% ethanolic solution to form aqueous phase. The resultant solution was heated at 65°C to ensure the phase transition of the lipid-bi-layer, when mixed further. After that, Docetaxel containing PEG: PCL solution was added to the preheated lipid solution via dropwise method at 1 mL/min flow rate under vigorous mixing at 200 to 2000 rpm for at least 0.5 to 2.5 h to ensure a complete evaporation of the organic solvent and maximum encapsulation of Docetaxel in PLHNCs. Furthermore, PLHNCs suspension was introduced to 1 to 6 extrusion cycles with laboratory manual extruder (Avestin LF-1) to improvise the encapsulation efficiency as well as the size distribution.

The developed formulation of Docetaxel hybrid nanocarriers was subjected for the complexation with shRNA pDNA for 15-45 mins to obtain the dual drug-gene-loaded hybrid nanocarriers. The positively charged lipid (i.e. DOTAP) of the Docetaxel PLHNCs makes complexation with negatively charged shRNA plasmid when incubated for 45 min. Incubation was conducted at 20 °C, 25 °C and 37 °C with various N/P ratios of cationic lipid (DOTAP) in hybrid nanocarriers to achieve the highest complexation efficiency. Similarly, ABCB1 shRNA-complexed hybrid nanocarriers without Docetaxel were also prepared using the same lipid composition for in vitro tests. Folate targeted D-sh-PLHNCs have been formulated using folic acid conjugated DSPE-PEG₂₀₀₀ in the formulation.

5.3.2 Preliminary screening study for formulation and process parameters

PLHNCs were formulated using single step nanoprecipitation followed by extrusion. polymer selection, amount of polymer, polymer to lipid ratio, lipid composition, drug input

was identified as formulation factors that may affect the quality target profile. While stirring time, stirring speed, extrusion cycle, complexation time was identified as process parameters that may alter quality profile of product. Preliminary screening is a control strategy that includes the material attributes and process parameters identified as potentially high-risk variables during the initial risk assessments. A Docetaxel and shRNA PLHNCs formulation is expected to provide a better therapeutic index due to carrier facilitated intracellular transportation as well as the targeting effect. For these reasons, the target profile of the intended Docetaxel PLHNCs is: (1) relatively high drug encapsulation efficiency (2) particle size below 200 nm and (3) sufficient stability on storage.

5.3.3 Selection of polymer

Polymeric nanoparticles were formed by Single step nanoprecipitation in which different synthetic polymers (i.e. Polycaprolactone, polylactic acid, PLGA, PEG-PCL, PEG-PLA) were dissolved in suitable solvent along with 5 % w/v of Docetaxel. Resulting organic phase was injected in aqueous phase containing Poloxamer 407 as surfactant with concentration of 0.5% w/v as laboratory developed method. Organic solvent was allowed to evaporate and nanoparticle drug suspension was obtained.

Table 5-3 Selection of polymer

Polymer (5 mg/ml)	Size (nm)	PDI	Entrapment Efficiency (%)	Zeta potential
Polycaprolactone (PCL)	162.5 ± 2.5	0.316 ± 0.12	36.1 ± 2.1	-11.6 ± 2.8
Polylactic acid (PLA)	152.5 ± 1.4	0.219 ± 0.28	32.9 ± 1.8	-22.1 ± 1.3
Poly D,L-lactic-co-glycolic acid (PLGA) (75:25)	198.6 ± 1.8	0.521 ± 0.32	28.6 ± 1.5	-38.4 ± 2.1
Poly D,L-lactic-co-glycolic acid (PLGA) (50:50)	168.7 ± 7.1	0.214 ± 0.16	43.1 ± 1.2	-13.1 ± 1.8
Polyethylene glycol - Polycaprolactone (PEG-PCL)	62.2 ± 2.5	0.125 ± 0.12	52.9 ± 3.1	-12.8 ± 1.2
Polyethylene glycol -Polylactic acid (PEG-PLA)	59.2 ± 8.2	0.112 ± 0.15	41.6 ± 2.4	-16.4 ± 1.8

From various polymers, PEG-PCL was selected for the preparation of PLHNCs on the basis of encapsulation efficiency, size and zeta-potential. PEG-PCL shows the highest entrapment of Docetaxel among all the polymers shown in Table 5-3. The highest entrapment

of Docetaxel in PEG-PCL was might be due to the lower Tg of PEG-PCL (-60°C) which results in quick self-assembly of nanoparticle in aqueous phase. Even particle size of the PEG-PCL nanoparticles was favouring the desired particles size, hence PEG-PCL was chosen for the further optimization.

5.3.4 Effect of polymer concentration on encapsulation efficiency and particle size:

As shown in Table 5-4, increasing the concentration of PEG-PCL (Di-block co-polymer) resulted in increased encapsulation efficiency of Docetaxel. At high polymer concentration, the internal core volume for drug encapsulation was high that led to a higher encapsulation efficiency. Drug encapsulation was solely dependent on hydrophobic polymeric core as well as the presence of lipid monolayer at the polymer lipid interface. At low polymer concentration, higher amount of free drug was reported, which showed insufficient hydrophobic core to entrap drug. With increasing concentration of polymer, gradual increase in entrapment efficiency and particle size was noted. After 10 mg/mL polymer concentration, no significant increment in drug encapsulation was observed. These effects explain another phenomenon that there could be an inverse relation between drug concentration and drug encapsulation after saturation of the hydrophobic core. As the polymer concentration increased, zeta potential of the PLHNCs shifted from positive to negative charge due to negative charge of the PEG-PCL. Drug input was taken as constant 5 % w/v to evaluate the effect of polymer concentration on encapsulation efficiency. L/P ratio (Lipid to polymer ratio) was taken at 5 % during the evaluation of polymer effect to avoid such influence of the lipid layer on the drug encapsulation.

Table 5-4 Effect of polymer concentration on Docetaxel encapsulation

Sr. No	Polymer concentration (mg/mL)	Entrapment efficiency (%)	Size (nm)	Zeta potential (mv)
1	2	36.9 ± 1.5	56.1 ± 1.2	7.8 ± 2.1
2	4	46.4 ± 1.5	61.1 ± 2.6	2.8 ± 2.1
3	6	52.2 ± 1.5	78.1 ± 2.5	-2.1 ± 1.6
4	8	59.7 ± 2.1	78.5 ± 3.2	-7.8 ± 1.2
5	10	68.6 ± 1.9	89.1 ± 1.8	-9.3 ± 2.3
6	12	69.4 ± 1.6	101.1 ± 1.2	-14.5 ± 2.1

5.3.5 Effect of lipid to polymer ratio on drug encapsulation and particle size

From Table 5-5, it is clear that the percentage weight ratio of lipid/polymer could achieve Docetaxel encapsulation above 80 %, between the range of 20 to 30%. Above 30% weight ratio, PDI was much wider, particle size ranging more than 200 nm, and formulation

showed two peaks of separate size distributions as seen in Figure 5-1. These findings suggested the formation of liposomes due to excessive lipids. To explain this phenomenon, DPPC as primary lipid needs to come into the picture. 85% of lung surfactant is composed of 16 carbon chain unsaturated fatty acids which have a very high resemblance with DPPC (3). From the data provided by the manufacturer, we have found that critical micellar concentration for the DPPC is ~0.4 mg/mL. Hence, if the concentration of the lipid in the formulation exceeded CMC then excessive lipid above CMC may form separate liposomes which would not be desired. Even a higher zeta potential value of 30 % L/P ratio suggests the formation of separate liposomes (due to excessive lipids) which contributes to the more cationic charge in formulations. Conversely, the lower L/P ratio shows a sudden fall in the zeta potential was noted, as there is a paucity of primary and secondary lipids that can cover the polymer core surface. Hence, during low L/P percentage, zeta potential of PLHNCs closely resemble to the zeta potential of bare PEG-PCL nanoparticles (-11.2 mV). The negative zeta potential value signifies the incomplete lipid coat over the polymeric core. Due to these reasons, for further study, we optimized 25 % L/P ratio as further increasing L/P ratio showed no notable contribution in the encapsulation efficiency. Drug input percentage was taken at 5 % w/v to avoid the influence on encapsulation efficiency while optimizing lipid to polymer percentage. Concentration of polymer was taken as 10 mg/ml as per optimization in section 5.3.4.

Table 5-5 Effect of L/P ratio on Docetaxel encapsulation

Sr. No.	L/P percentage Ratio (%)	Mole fraction (DPPC: DOTAP: DSPE-PEG)	Entrapment (%)	Size (nm)	Zeta potential (mV)	PDI
1	5	50:30:20	68.6 ± 1.9	89.1 ± 1.8	-9.3 ± 2.3	0.124 ± 0.014
2	10	50:30:20	76.2 ± 2.1	95.4 ± 1.6	-1.2 ± 2.4	0.162 ± 0.012
3	15	50:30:20	79.8 ± 1.5	97.5 ± 2.1	8.9 ± 1.9	0.181 ± 0.014
4	20	50:30:20	83.5 ± 3.1	108.2 ± 1.1	15.2 ± 1.6	0.124 ± 0.021
5	25	50:30:20	95.2 ± 1.9	115.4 ± 2.4	24.8 ± 2.1	0.118 ± 0.011
6	30	50:30:20	96.3 ± 1.6	125.5 ± 3.8	32.5 ± 1.8	0.564 ± 0.021
7	35	50:30:20	97.2 ± 2.1	512.5 ± 4.1	54.6 ± 2.8	0.798 ± 0.032

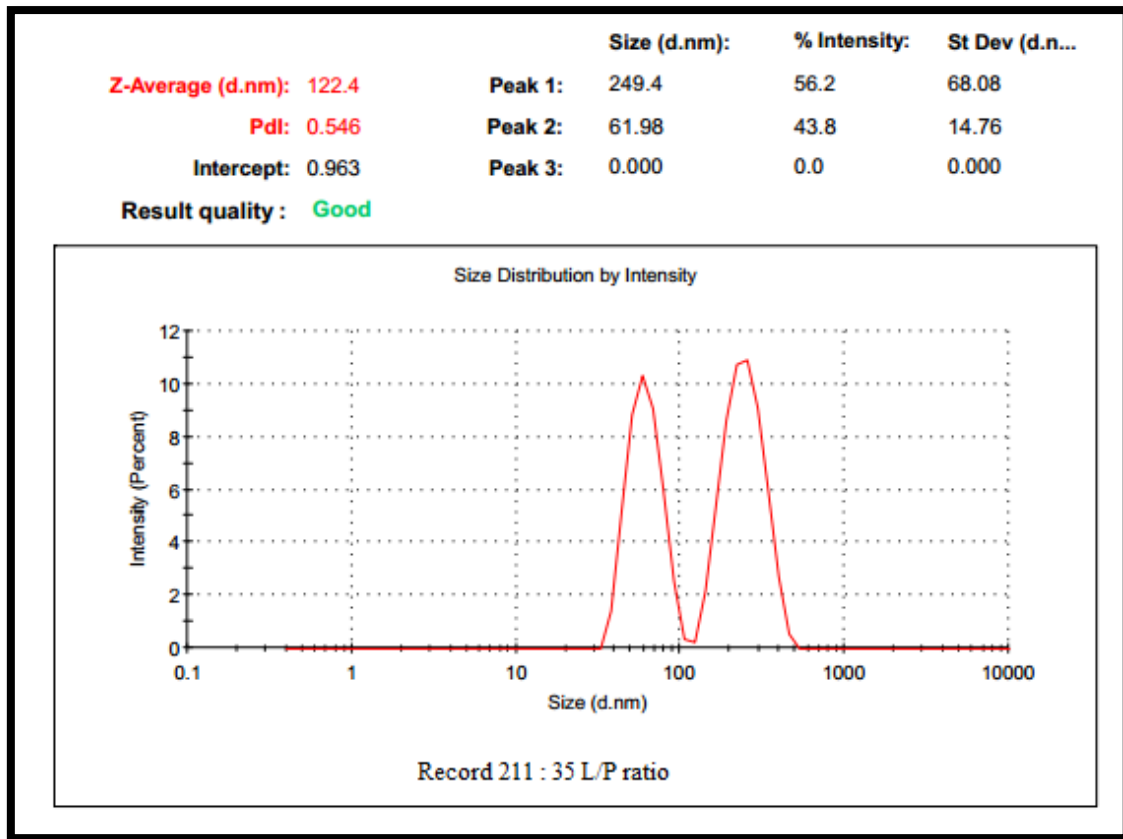


Figure 5-1 Particle size distribution of L/P ratio 35

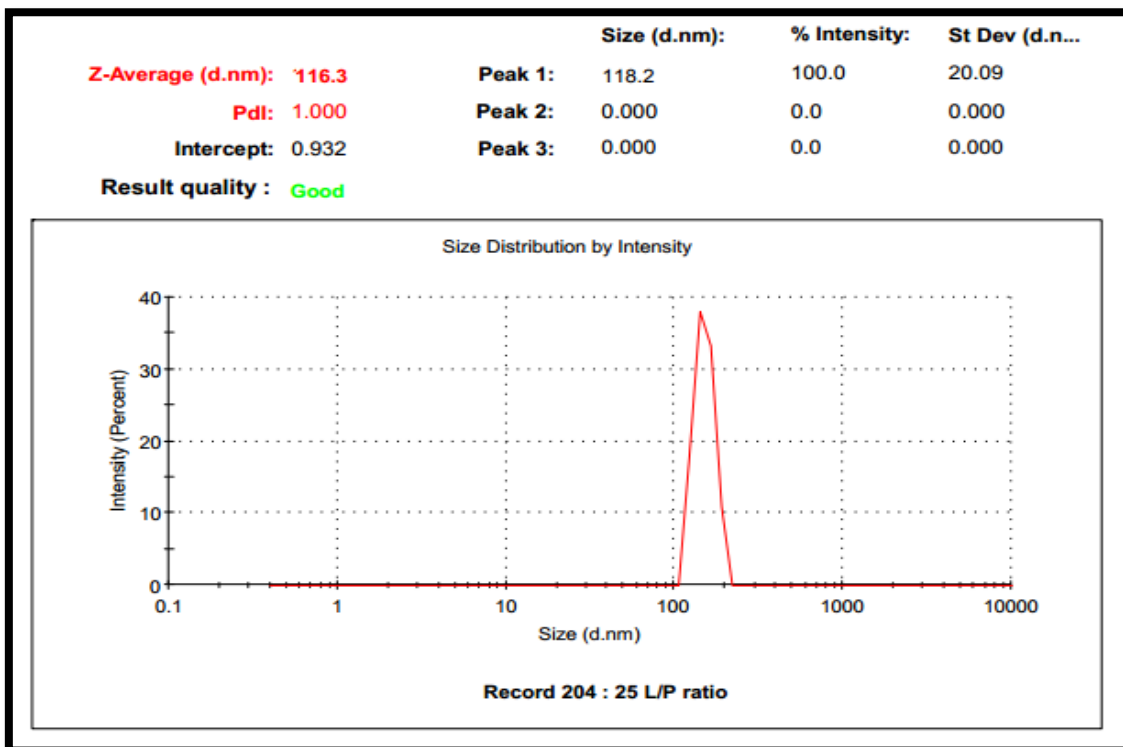


Figure 5-2 Particle size distribution of L/P ratio 25

5.3.6 Effect of drug input on encapsulation efficiency and particle size

As portrayed in Table 5-6, As the initial drug input was increased from 5% to 10%, percentage drug encapsulation remained same. Though, as the drug input further increased to 15 %, there was only ~73.2 % encapsulation of Docetaxel which showed a reduction in the encapsulation efficiency. Polymer concentration and L/P percentage was taken 10 mg/ml and 25 % respectively as per optimization in section 5.3.4 and 5.3.5.

Table 5-6 Effect of drug input on Docetaxel encapsulation

Sr. No	Drug input (% w/w of polymer)	Entrapment Efficiency (%)	Size (nm)	Zeta potential (mV)
1	5	95.2 ± 1.9	115.4 ± 2.4	24.8 ± 2.1
2	10	96.5 ± 1.6	118.2 ± 1.8	26.2 ± 1.8
3	15	73.2 ± 1.2	124.3 ± 3.5	32.6 ± 2.4

5.3.7 Effect of lipid composition ratio on docetaxel encapsulation, particle size of PLHNCs and complexation efficiency of shRNA

Lipid composition may affect the encapsulation efficiency of PLHNCs, as the outer lipid shell can act as a fence to polymeric inner core which further prevents drug leakage during the storage. Hence, in this research, DPPC was used as primary lipid as it has a considerable biocompatibility with lung fluids and exhibits a major ratio in the composition of lipids. DOTAP has been used as cationic lipid of which cationic heads make a complex with anionically charged ABCB1 shRNA plasmid molecule. Amount of cationic lipid in the lipid composition affects the complexation efficiency of shRNA pDNA. As the amount of cationic lipid increased in the PLHNCs, zeta potential shifted from negative to positive as shown in Table 5-7. The zeta potential of the resultant D-sh-PLHNCs were lesser compared to blank PLHNCs (30.4 mV ± 1.3) for N/P ratio of 2.5 suggest the complexation of anionically charged shRNA pDNA to cationic lipid. The reduced zeta potential of the cationic lipid (as shown in Table 5-7) is due to the efficient complexation of the anionically charged molecule. From the Table 5-7 it is clearly seen that twice molar excess of cationic nitrogen of DOTAP was required over phosphates of the shRNA, which satisfies an N/P ratio of 2.5. N/P ratio higher than 2.5 could not show any significant enhancement in the complexation of ABCB1 shRNA plasmid. Furthermore, it can be concluded that with increasing concentration of DOTAP over 25-mole fraction, there was a slight change over the complexation efficiency. During the lipid composition ratio optimization, encapsulation of Docetaxel remained ~95% in all formulations. Hence, it can be stated that the change in the lipid composition ratio did not show any significant change in Docetaxel encapsulation in PLHNCs. Polymer concentration, Lipid to

polymer percentage and drug input are taken 10 mg/ml, 25 % and 10 % as per optimization in section 5.3.4, 5.3.5 and 5.3.6.

N/P ratio was calculated using the following equation:

$$\left[\frac{N}{P}\right] = \frac{\left[\frac{\text{weight of cationic lipid}}{\text{molecular wt of lipid}}\right] * (\text{charge per 1 lipid molecule})}{\left[\frac{\text{weight of pDNA to be taken}}{\text{molecular weight pDNA}}\right] * (\text{charge per 1 pDNA molecule ie } 9432 * 2)}$$

Table 5-7 Effect of lipid composition ratio on the complexation efficiency of shRNA and Docetaxel encapsulation

Sr. No.	Mole fraction (DPPC: DOTAP: DSPE-PEG)	N/P ratio	Docetaxel Entrapment Efficiency (%)	Complexation efficiency of shRNA (%)	Zeta potential (mV)	Size ± SD (nm)
1	80:5:15	0.5	96.3 ± 1.8	12.2 ± 2.1	-23.5 ± 2.1	119.2 ± 1.8
2	75:10:15	1.0	95.6 ± 2.1	23.6 ± 3.5	-5.6 ± 3.1	118.6 ± 1.2
3	70:15:15	1.5	96.4 ± 1.9	38.6 ± 1.5	6.8 ± 2.4	121.8 ± 1.1
4	65:20:15	2.0	94.2 ± 2.6	72.4 ± 1.2	11.6 ± 1.8	119.7 ± 1.6
5	60:25:15	2.5	95.6 ± 1.9	96.2 ± 1.4	22.6 ± 2.6	115.4 ± 1.2
6	55:30:15	3.0	94.6 ± 2.4	98.1 ± 1.2	31.9 ± 1.2	117.2 ± 1.4
7	50:35:15	3.5	96.5 ± 2.6	98.9 ± 4.2	39.6 ± 3.4	116.8 ± 1.5

5.3.8 Effect of process on encapsulation efficiency and particle size

After injection, stirring was performed for a maximum period of 2 h. Furthermore, the formulation was subjected to various extrusion cycle using laboratory manual extruder (Avestin LF-1). This can be further defined by the encapsulation efficiency and particle size of the PLHNCs. Preliminary screening of process parameters has been shown in Table 5-8.

Table 5-8 Effect of process parameters on encapsulation of Docetaxel, Complexation of shRNA plasmid and particle size as well as poly dispersity index (PDI).

Effect of process parameters on encapsulation efficiency of Docetaxel			
Stirring speed (rpm)	Encapsulation efficiency (%)	Particle size (nm)	PDI
200	71.65 ± 1.2	220.54 ± 2.9	0.154 ± 0.024
500	82.67 ± 2.4	112.5 ± 2.4	0.201 ± 0.028
1000	79.56 ± 1.3	96.61 ± 1.6	0.229 ± 0.031
1500	87.44 ± 1.8	92.54 ± 1.4	0.238 ± 0.024
2000	82.49 ± 2.1	84.29 ± 1.3	0.245 ± 0.018
2200	85.32 ± 1.6	82.65 ± 1.1	0.249 ± 0.012

Stirring time (H)	Encapsulation efficiency	Particle size	PDI
0.2	86.54 ± 2.1	264.54 ± 1.1	0.249 ± 0.034
0.5	88.64 ± 1.2	124.57 ± 1.6	0.265 ± 0.025
1	84.61 ± 1.4	124.35 ± 2.3	0.311 ± 0.028
1.5	84.21 ± 2.2	128.64 ± 2.1	0.289 ± 0.011
2	89.54 ± 1.3	124.94 ± 1.5	0.345 ± 0.021
2.5	78.65 ± 1.7	79.21 ± 1.4	0.345 ± 0.018
Cycles	Encapsulation efficiency	Particle size	PDI
1	89.54 ± 2.4	124.94 ± 3.4	0.348 ± 0.014
2	86.23 ± 1.4	112.5 ± 2.8	0.345 ± 0.016
3	89.35 ± 1.1	108.54 ± 1.8	0.256 ± 0.021
4	91.97 ± 1.6	98.35 ± 1.2	0.198 ± 0.024
5	93.54 ± 2.1	91.4 ± 1.4	0.156 ± 0.012
6	91.47 ± 1.9	89.76 ± 2.2	0.105 ± 0.011
Effect of process on complexation efficiency of shRNA pDNA			
Incubation time	Complexation efficiency	Particle size	PDI
15	65.84 ± 2.4	92.76 ± 2.1	0.125 ± 0.016
30	85.14 ± 1.7	96.54 ± 1.2	0.164 ± 0.021
45	86.26 ± 1.9	98.21 ± 1.6	0.129 ± 0.011
Incubation temperature	Complexation efficiency	Particle size	PDI
20	71.29 ± 1.6	98.24 ± 2.2	0.154 ± 0.018
25	89.51 ± 1.5	98.69 ± 1.7	0.148 ± 0.023
37	91.25 ± 2.1	99.13 ± 1.1	0.131 ± 0.017

Process parameters i.e., stirring speed and stirring time was chosen as per the encapsulation efficiency and complete removal of solvent from PLHNC suspension. Extrusion cycles from 1 to 3 was not seen to improve the PDI of the formulation hence higher extrusion cycles were tried to improve PDI and encapsulation efficiency. When shRNA pDNA was complexed for 45 mins at 37⁰ C gave highest complexation up to 91 %.

5.4 RISK ASSESSMENT

Preliminary studies were performed to identify the potential risks of the formulation as well as process parameters and related causes. Particle size and entrapment efficiency were identified as quality attributes for the development. After the preliminary analysis, seven key variables were identified that affect the quality attributes and screened in subsequent studies.

5.5 QUALITY BY DESIGN

To achieve the above quality profile, a systematic QbD method was used. A comprehensive QbD study (4, 5) should comprise of the following four key elements: (1) define target quality of product profile (goals) based on scientific foreknowledge and acceptable in vivo relevance;

(2) design product and manufacturing techniques to gratify the pre-defined profile; (3) recognise critical quality attributes, processing parameters, and sources of variability to acquire the design space; and (4) control manufacturing techniques to generate consistent product quality over period through operating condition within the established design space (the margin of process and/or formulation variables that have been illustrated to provide assurance of quality), thus guaranteeing that quality is maintained into the product (ICH Q8). In addition, risk analysis narrowed down seven factors to elevated risk factors that may influence the efficiency of PLHNCs drug encapsulation and particle size. For this purpose, two experimental designs were used. First, a Plackett–Burman screening design (6) was used to identify the most significant factors affecting Docetaxel encapsulation and particle size of developed PLHNCs. Next, a Box-behnken (BBD) was used in the response surface study to obtain the exact relationship between the Docetaxel encapsulation and various factors (that have been identified in the screening study). This model uses an articulated factorial design of centre points which is enhanced with a community of axial points that enables curvature calculation and also allows the design to be rotatable. (7). After obtaining the response surface the optimal formulation and process conditions were identified. Further experimental tests were performed to test the robustness and accuracy of the generated model. A desired batch of the PLHNCs were exposed to shRNA pDNA complexation to developed Docetaxel and shRNA pDNA loaded PLHNCs.

5.5.1 Plackett-Burman design for screening study (Primary design):

The results of preliminary study was useful to assist formulation-related and process-related parameters and to understand the source of variables in order to improve the quality of product to assist formulation and process. Key product attributes recognized as particle size and encapsulation efficiency were evaluated for different variables. The goals of applying design were to achieve the highest encapsulation of Docetaxel along with the narrow particle size distribution.

Table 5-9 Variables and levels selected for preliminary study

Factor	Name	Unit	Low actual	High actual
A	Polymer concentration	mg/ml	5	10
B	Lipid/Polymer ratio	%	5	30
C	drug input percentage	%	5	15
D	Stirring speed	rpm	500	2000
E	Stirring time	H	0.5	2
F	Sonication time	s	30	120
G	Extrusion cycle	-	3	6

The Plackett-Burman study design has been implemented for screening of various formulation and process-related parameters i.e., polymer concentration (mg/mL) (Factor A), lipid/polymer percentage (%) (Factor B), drug input percentage (%) (Factor C), stirring speed (RPM) (Factor D), stirring time (h) (Factor E), sonication time (S) (Factor F), extrusion cycle (Nos) (Factor G) and its impact on encapsulation efficiency and particle size distribution. These parameters were assessed to be of high importance in consideration with other factors based on different trials. For the screening study, 7 factors in the different columns were evaluated at the lowest level (-1) and highest level (+1) which is shown in Table 5-10. The lowest and the highest values that can be used for the formulation of PLHNCs and can be selected on the basis of preliminary study results. The encapsulation of the design matrix batch were lesser compared to preliminary studies due to randomization between highest and lowest range of the factors come together which impact the results of encapsulation efficiency.

Table 5-10 Design Matrix of Plackett Burman design

Run	Factor A Polymer conc. (mg/mL)	Factor B Lipid to polymer percentage Ratio	Factor C Drug input percentage (%)	Factor D Stirring speed (rpm)	Factor E Stirring time (h)	Factor F Sonication time (s)	Factor G Extrusion cycle	Response 1 Encapsulation efficiency	Response 2 Particle size
1	10	5	15	2000	0.5	120	6	67.98	77.84
2	5	30	5	2000	2	30	6	49.54	61.02
3	5	5	5	500	0.5	30	3	45.78	64.25
4	10	30	5	500	0.5	120	3	75.28	84.25
5	10	5	5	500	2	30	6	62.57	72.54
6	10	5	15	2000	2	30	3	68.94	78.69
7	5	5	15	500	2	120	3	43.54	54.81
8	5	30	15	500	2	120	6	52.04	63.41
9	10	30	15	500	0.5	30	6	78.54	87.39
10	10	30	5	2000	2	120	3	74.95	84.61
11	5	30	15	2000	0.5	30	3	51.24	62.01
12	5	5	5	2000	0.5	120	6	46.21	57.23

5.5.1.1 ANOVA for encapsulation efficiency (Factorial model)

Multi-linear regression analysis and ANOVA (shown in Table 5-11) have been performed to analyse the data, and a series of Pareto charts were constructed to demonstrate the influence of each parameter on encapsulation efficiency.

Table 5-11 ANOVA on factorial model for encapsulation efficiency

Source	Sum of Squares	Degree of freedom	Mean Square	F-value	p-value (prob>F)
Model	1862.68	10	186.27	1884.99	0.0179
A-Polymer concentration	1150.92	1	1150.92	11647.05	0.0059
B-Lipid/Polymer ratio	81.96	1	81.96	829.38	0.0221
C-drug input percentage	8.49	1	8.49	85.89	0.0684
D-Stirring speed	9.63	1	9.63	97.42	0.0643
E-Stirring time	0.13	1	0.13	1.35	0.4523
F- Sonication time	10.86	1	10.86	109.93	0.0605
G-Freeze and thaw cycle	2.09	1	2.09	21.13	0.1364
AC	21.32	1	21.32	215.76	0.0433
AE	3.24	1	3.24	32.80	0.1100
CF	0.98	1	0.98	9.96	0.1953
Model statistics					
Standard deviation		0.31			
Mean		59.72			
R ²		0.9999			
Adeq Precision		116.291			

The Model F-value of 1884.99 implies the model is significant. There is only a 1.79% chance that a large "Model F-Value" could occur due to noise. Values of "Prob > F" less than 0.0500 indicate model terms are significant. In this case A, B, AC are significant model terms. Values greater than 0.1000 indicate the model terms are not significant. "Adeq Precision" measures the signal to noise ratio. A ratio greater than 4 is desirable. Ratio of 116.291 indicates an adequate signal. This model can be used to navigate the design space. Hence we can conclude that polymer concentration (A), Lipid to polymer ratio (B) and Drug input percentage (C) are the potential factors that affect the encapsulation efficiency of the PLHNCs. Further there are significance interactions between Factor A and C which is justified by following box-beneken design. Other interactions between factor AE and factor CF are not found significant hence it has no impact on the encapsulation efficiency of PLHNCs.

5.5.1.2 Influence of factors on encapsulation efficiency (Pareto chart)

The Pareto chart was used as a graphical tool to manage model selection for two-level factorial designs. As represented in Figure 5-3, factor A (Polymer concentration) had crossed the Bonferroni limit, it possesses the utmost importance for increasing encapsulation efficiency. Another factor B (L/P ratio) and C (Drug input) may have an intermediate effect on the encapsulation efficiency as these factors have the ability to cross the t-critical value limit. The t-critical value limit was considered as a lower limit for the factors that affect the response. Further, there were significant interactions between factor A and C, which were justified by

following the Box-Behnken design. Other interactions between factor AE and factor CF were not found significant, hence it had no impact on the encapsulation efficiency of PLHNCs.

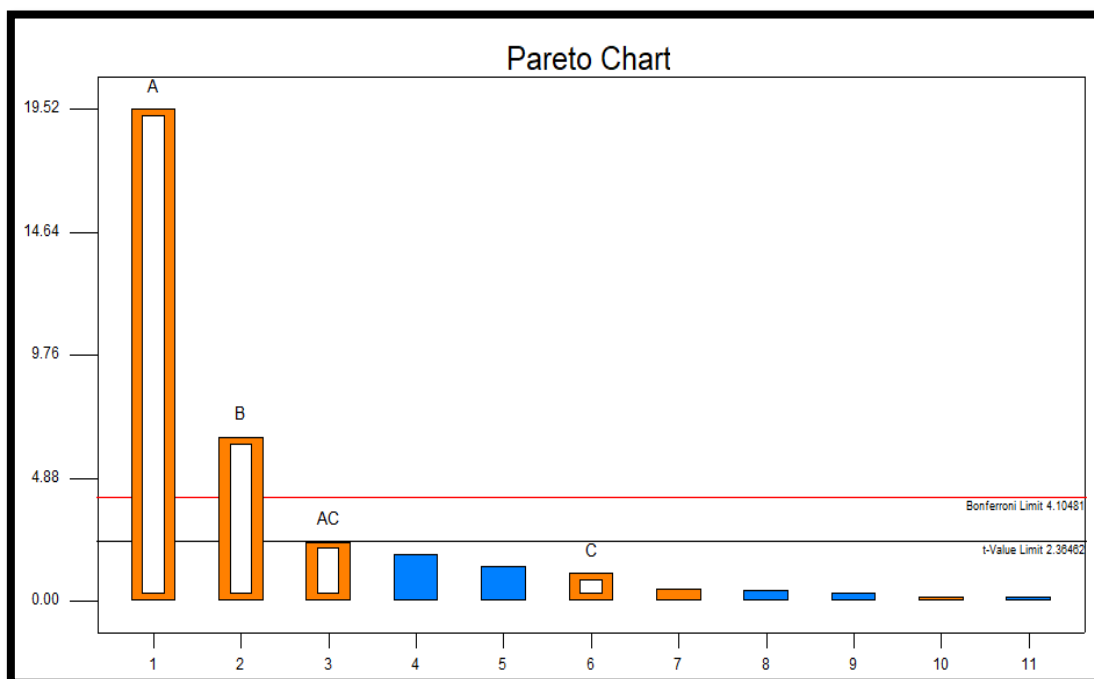


Figure 5-3 Pareto Chart for the selected factorial model of Encapsulation efficiency

The Pareto chart depicted that all the independent variables concentrations of polymer, lipid to polymer percentage ratio and drug input percentage have exerted a most significant effect (Above t-value limit) on the response variables.

5.5.1.3 ANOVA for particle size (Factorial model)

Multi-linear regression analysis and ANOVA (shown in Table 5-12) have been performed to analyse the data, and a series of Pareto charts were constructed to demonstrate the influence of each parameter on the particle size of PLHNCs.

Table 5-12 ANOVA on factorial model for encapsulation efficiency

Source	Sum of Squares	Degree of freedom	Mean Square	F-value	p-value (prob>F)
Model	1464.86	9	162.76	47.28	0.0209
A-Polymer concentration	965.47	1	965.47	280.48	0.0035
B-Lipid/Polymer ratio	115.10	1	115.10	33.44	0.0286
C-drug input percentage	5.34	1	5.34	6.66	0.2353
D-Stirring speed	14.53	1	14.53	4.22	0.1763
E-Stirring time	67.53	1	67.53	1964	0.0673
F- Sonication time	29.71	1	29.71	8.63	0.0990
G-Freeze and thaw cycle	0.051	1	0.051	0.015	0.9145
AD	9.28	1	9.28	11.41	0.0776
AG	18.73	1	18.73	5.44	0.1449
EG	6.16	1	6.16	1.79	0.3128
Model statistics					

Standard deviation	1.86
Mean	70.67
R ²	0.995
Adeq Precision	19.026

The Model F-value of 47.28 implies the model is significant. There is only a 2.09% chance that a "Model F-Value" this large could occur due to noise. Values of "Prob > F" less than 0.0500 indicate model terms are significant. In this case independent variable A and B are significant model terms. Values greater than 0.1000 indicate the model terms are not significant. Adequate precision ratio of 19.026 (greater than 4) indicates an adequate signal. This model can be used to navigate the design space. Hence, we can conclude that polymer concentration (A) and Lipid to polymer ratio (B) are the potential factors that affect the particle size of the PLHNCs. And there is no cross-interaction between other factors that can lead to significant change in particle size of PLHNCs. Further, effect of two variable on particle size were screened using box-behnken design.

5.5.1.4 Influence of factors on particle size (Pareto chart)

As observed in Figure 5-4, factor A (i.e., polymer concentration) has crossed the Bonferroni limit, it possesses the utmost importance for increasing the particle size. Another factor B (i.e., L/P ratio) may have an intermediate effect on the encapsulation efficiency, since that factors have the ability to cross the t-critical value limit. Process parameters may have a significant effect on the particle size but for the quality target profile (less than 200 nm) within range of the design, different process doesn't give any significant change in particle size. Moreover, negligible effect of process on PLHNCs target profile justifies the self-assembly system of the manufacturing. Further, there were no significant interactions found between any factors.

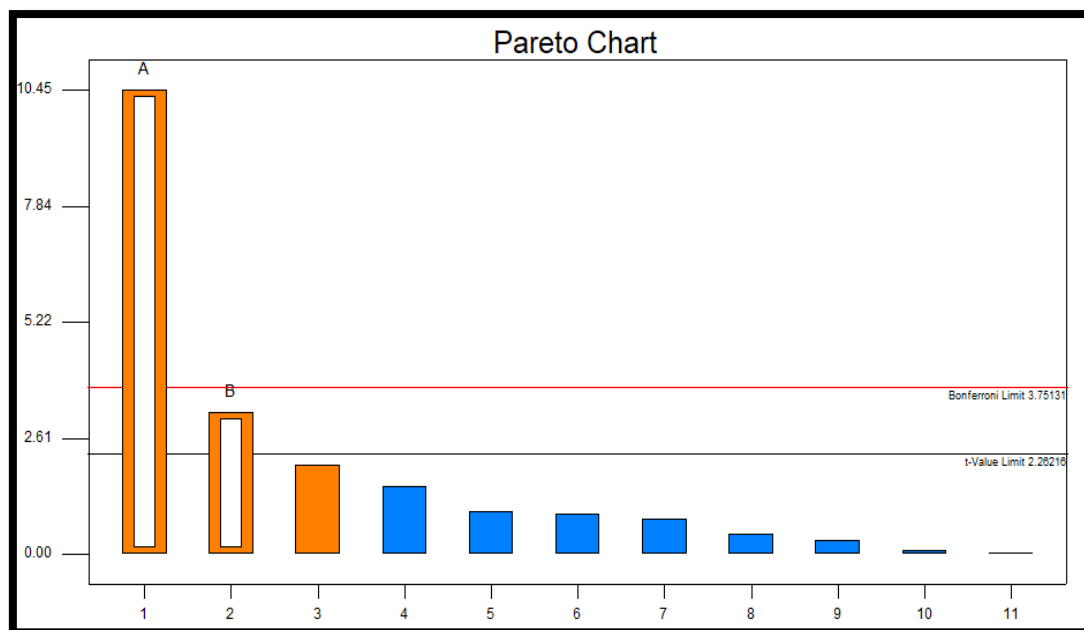


Figure 5-4 Pareto Chart for a selected factorial model of particle size

The Pareto chart depicts that independent variables A (i.e., polymer concentration) and B (i.e., lipid to polymer percentage) have a significant impact on the particle size of the PLHNCs (above t-value limit).

5.5.2 Box-behnken design for point prediction (Secondary design)

Based on the results of the primary factor screening design, three variables (i.e., polymer concentration, lipid to polymer percentage and drug input percentage) were selected for further optimization (As shown in Table 5-13) using the response surface method, more specifically Box-Behnken design. The Box-Behnken design will help to analyze the influence of factors on the pharmacokinetic response and characteristics of the PLHNCs. The three-factorial two-level Box-Behnken design, which consists of a set of points located at the midpoint of each end and the replicated central point of the multi-dimensional cube was used to obtain the polynomial models. A suitable design (As shown in Table 5-14) has been developed that integrates independent variable and generates the final equations that can result into a theoretical outcome for the response. The best suitable model has been selected for the point prediction and surface response curve for each response using ANOVA. The encapsulation of the design matrix batch were lesser compared to preliminary studies due to randomization between highest and lowest range of the factors come together which impact the results of encapsulation efficiency.

Table 5-13 Variables and levels selected on the basis of primary design

Independent variables	Unit	Levels	
		-1	+1
A: Polymer concentration	mg/ml	5	15
B: Lipid to polymer ratio	Percentage	5	30
C: Drug input percentage	Percentage	5	15
Dependent variables		Unit	
1: Encapsulation Efficiency		Percentage	
2: Particle size		nm	

Table 5-14 Design matrix of Box-Behnken design

Run	Factor A: Polymer concentration (mg/mL)	Factor B: Lipid to polymer percentage (%)	Factor C: Drug input percentage (%)	Response 1: Encapsulatio n efficiency (%)	Response 2: Particle size (nm)
1	7.50	17.50	10.00	71.49	82.46
2	7.50	17.50	10.00	80.91	81.92
3	10.00	17.50	5.00	79.25	89.23
4	5.00	17.50	5.00	67.42	76.97
5	7.50	5.00	15.00	69.54	79.86
6	5.00	30.00	10.00	67.94	78.23
7	5.00	17.50	15.00	65.24	75.81
8	7.50	17.50	10.00	72.99	83.47
9	10.00	5.00	10.00	79.21	88.14
10	7.50	17.50	10.00	72.94	83.56
11	10.00	30.00	10.00	81.49	92.51
12	7.50	5.00	5.00	71.64	81.02
13	5.00	5.00	10.00	62.54	72.91
14	10.00	17.50	15.00	79.86	90.05
15	7.50	17.50	10.00	74.61	84.21
16	7.50	30.00	15.00	64.95	85.42
17	7.50	30.00	5.00	75.83	86.14

5.5.2.1 Statistical analysis of response (dependent) variable 1: Encapsulation efficiency

5.5.2.1.1 ANOVA results of different models

Summary of the ANOVA results for different models as shown in Table 5-15 which depicts sequential p-values and Lack of Fit p-values along with Adjusted and Predicted R-squared values for different models.

Table 5-15 Summary of ANOVA results of different models for Encapsulation efficiency

Source	Sequential	Lack of fit	Adjusted R-squared	Predicted R-squared	Suggested model
	p-value	p-value			
Linear	0.6898	0.5658	0.6983	0.6026	
2FI	0.5889	0.6138	0.6735	0.4328	
Quadratic	0.0003	0.6421	0.9750	0.9332	Suggested
Cubic	0.6138	-	0.6372	-	Aliased

Highest polynomial showing the lowest p value (<0.05) along with highest Lack of Fit p-value (>0.1) was considered for model selection. Based on the criteria quadratic model was found to be best fitted to the observed responses. Special cubic and higher models were not suitable for prediction either due to low R-squared values and/or due to higher p value as compared to quadratic model (As shown in table Table 5-15). Quadratic and higher models were aliased indicating the confounding of the model terms when the other model implying that the predicted response would give the wrong idea of the actual response.

Table 5-16 ANOVA results of quadratic mixture model for encapsulation efficiency

Source	Sum of Squares	df	Mean Square	F Value	p-value Prob > F	
Model	445.97	9	49.55	70.34	<0.0001	significant
A-Polymer concentration	392.14	1	392.14	556.66	<0.0001	
B-lipid to polymer weight ratio	51.87	1	51.87	73.63	<0.0001	
C-Drug input percentage	0.62	1	0.62	0.87	0.3808	
AB	0.23	1	0.23	0.32	0.5891	
AC	0.98	1	0.98	1.39	0.2767	
BC	0.048	1	0.048	0.069	0.8008	
A ²	0.078	1	0.078	0.11	0.7497	
B ²	0.00006	1	0.0006	0.0009	0.9234	
C ²	0.0003	1	0.0003	0.0004	0.9497	
Residual	4.93	7	0.70			
Lack of Fit	1.55	3	0.52	0.61	0.6421	not significant
Pure Error	3.38	4	0.84			
Cor Total	450.90	16				
ANOVA Summary						
Parameters	Results		Parameters		Results	
Std. Dev.	0.84		R-Squared		0.9891	
Mean	83.05		Adj R-Squared		0.9750	
C.V. %	1.01		Pred R-Squared		0.9332	
PRESS	30.10		Adeq Precision		6.936	

The ANOVA table revealed that the effect of factors was significant and hence the model is significant for the entrapment efficiency. The F value was highest for the factor A (556.66), i.e., increasing polymer concentration would increase the entrapment of Docetaxel in linear manner. Other two factors such as lipid to polymer ratio (factor B) and drug input percentage (factor C) have low effect on encapsulation efficiency compared to polymer concentration which can also be observed from surface plots.

The Model F-value 70.34 implies that model is significant. There is only a 0.01% chance that a "Model F-Value" this large could occur due to noise. Values of "Prob > F" less than 0.0500 indicate model terms are significant. In this case A, B are significant model terms. Values greater than 0.1000 indicate the model terms are not significant. The "Lack of Fit F-value" of 0.61 implies the Lack of Fit is not significant relative to the pure error. Non-significant lack of fit is good hence we want the model to fit. The "Pred R-Squared" of 0.9332 is in reasonable agreement with the "Adj R-Squared" of 0.9750. "Adeq Precision" measures the signal to noise ratio. A ratio greater than 4 is desirable. Ratio achieved here is 6.936 which indicates an adequate signal. This model can be used to navigate the design space.

5.5.2.1.2 Model diagnostic plots for encapsulation efficiency

5.5.2.1.2.1 Normal residuals plot

The normal probability plot (normal plot of residuals) which shows whether the residuals follow a normal distribution or not and helps identify any specific patterns in the residuals indicative of requirement of transformations i.e. "S-shaped" curve, etc. Our normal plot of residuals for the current data follows a straight line, indicating no abnormalities. The data doesn't have to match up perfectly with the line. A good rule of thumb is called the "fat pencil" test. If you can put a fat pencil over the line and cover up all the data points, the data is sufficiently normal. In this case the plot looks to fit in fat pencil (As shown in **Figure 5-5**) hence our plot is considered as normal.

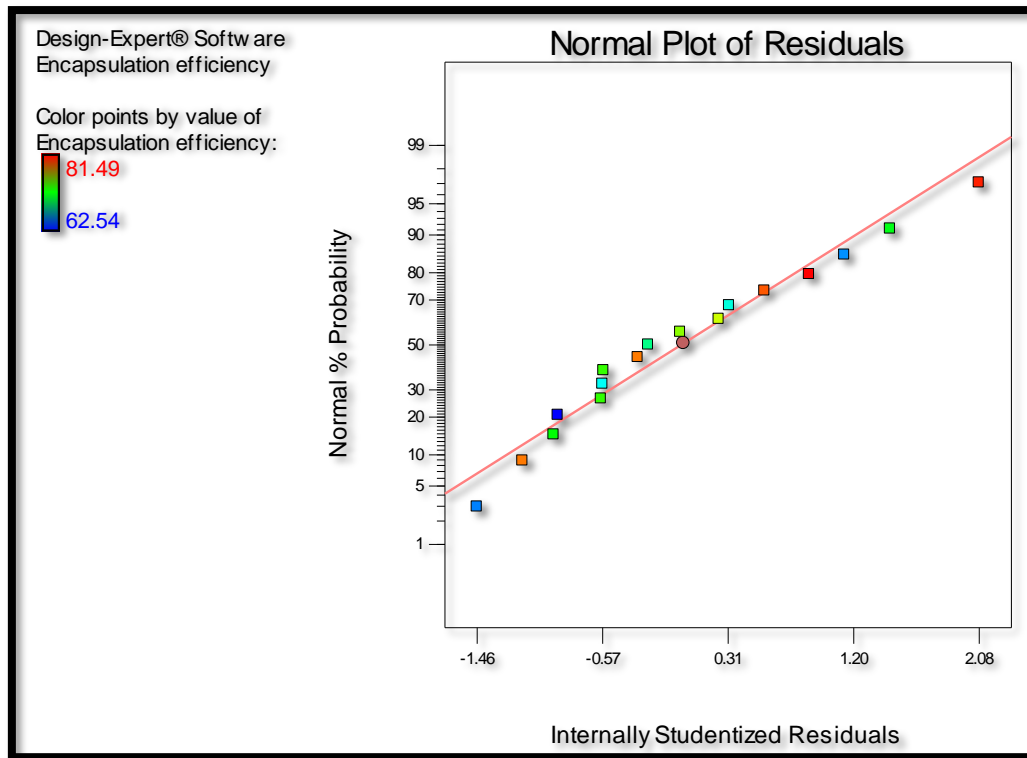


Figure 5-5 Normal plot of residuals for encapsulation efficiency

5.5.2.1.2.2 Residuals vs. predicted plot

Residuals vs. predicted response (ascending values) plot tests if variance is distributed over the design constantly i.e. variance is not associated with the factor values as megaphone patterns (pattern like sign horizontal cone $>$ or $<$) which indicate either decreasing or increasing residuals with increasing the factor values. This is a plot of the residuals versus the ascending predicted response values. The size of the residual should be independent of its predicted value. In other words, the vertical spread of the studentized residuals should be approximately the same across all levels of the predicted values. In this case (As shown in **Figure 5-6**) no horizontal cone shaped shape in the plot was recognized from the current data hence the variance is distributed all over the design constantly.

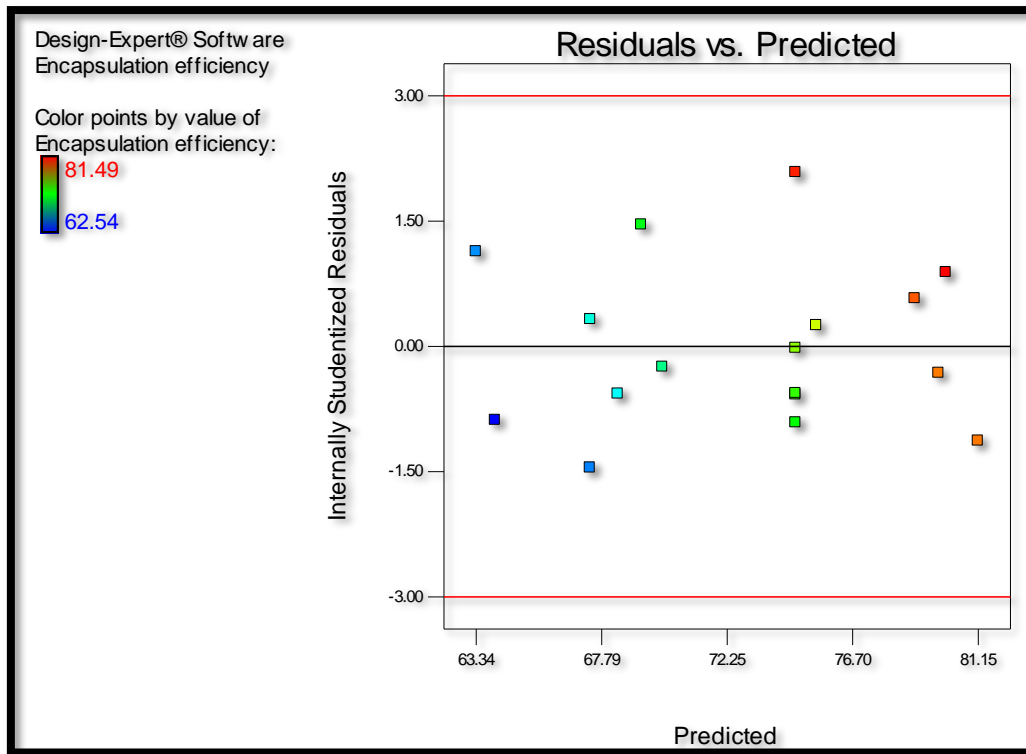


Figure 5-6 Residual vs. Predicted plot for encapsulation efficiency

5.5.2.1.2.3 Residual vs. Run order plot

The residuals against the experimental run order i.e., order in which the experiments have been carried out. The current plot (As shown in Figure 5-7) is having a random scatter of residuals which indicate there is no time dependent changes occurring in the residuals. In graph there is no downward or upward trend noticed hence it is confirmed that experiment will be done in random manner and selected model provide protection against any biased result in the design and point prediction.

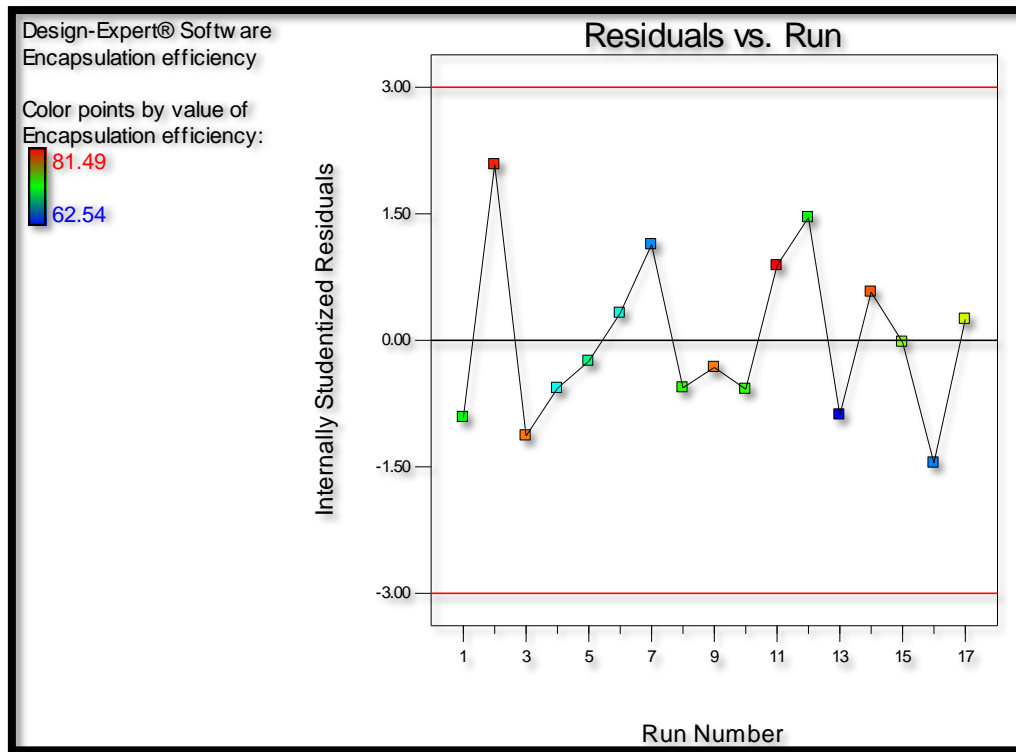


Figure 5-7 Residual vs. Run plot for encapsulation efficiency

5.5.2.1.2.4 Predicted vs. Actual plot

This plot shows correlation between the observed response values and actual response values. Hence plot from data shows (As seen in Figure 5-8) a straight line at 45° that indicates that model we have chosen for prediction of response are appropriate over all design matrix.

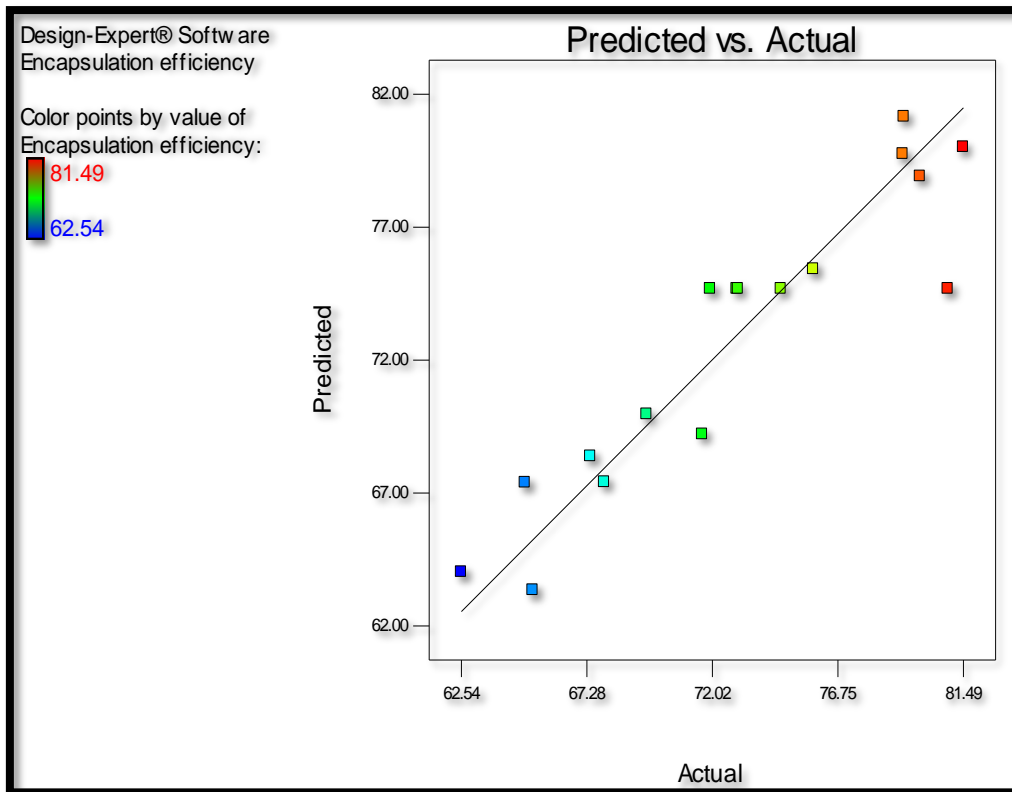


Figure 5-8 Predicted vs. Actual plot for the encapsulation efficiency

5.5.2.1.2.5 Box-cox plot for power transformation

Box-Cox plot of $\ln(\text{residuals sum of squares})$ vs. λ for power transformation helps to select any power transformation of observed response values required for fitting the model based on the best λ value and 95% confidence interval around it. Plot in Figure 5-9 shows the λ value of 1, which lies near the best λ value and within 95% confidence interval of it, indicating no requirement for any power transformation.

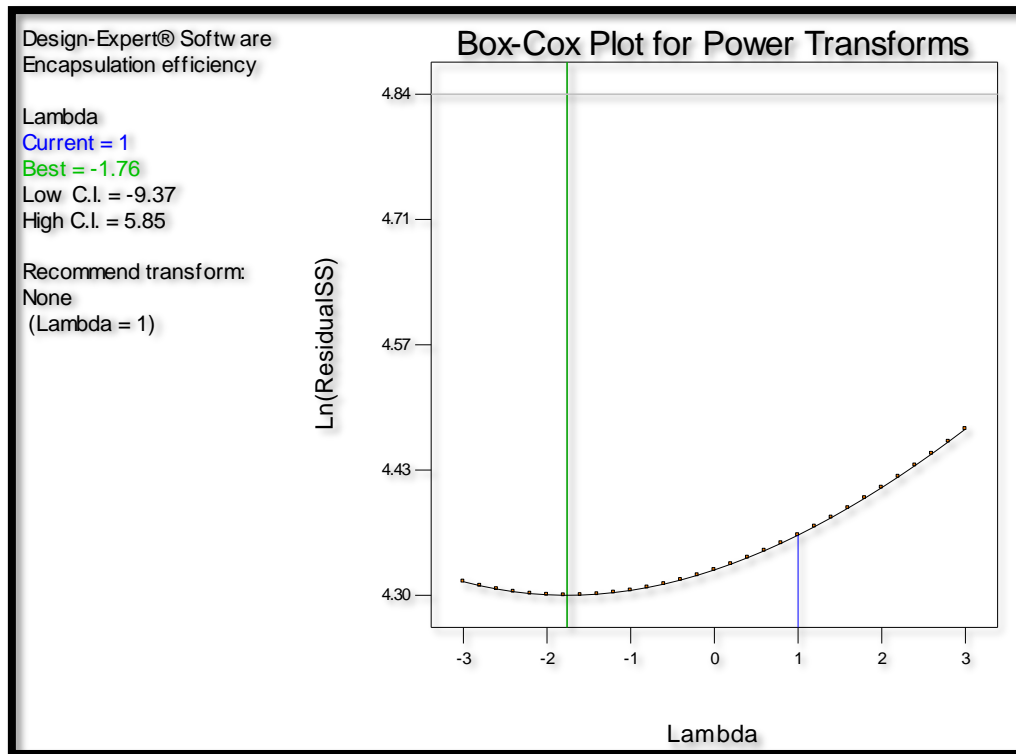


Figure 5-9 Box-Cox plot for power transformation for the encapsulation efficiency

5.5.2.1.2.6 Residual vs. Individual factor plots

Plot of residuals vs. any individual factor was evaluated to observe association between the variance associated with different levels of factor i.e. any specific trends (+ve or -ve curvatures) associated with increasing level of each factor. As it can be seen from the Figure 5-10, each factor shows a random scattering which indicates that model is effective in accounting for the variance for individual factor.

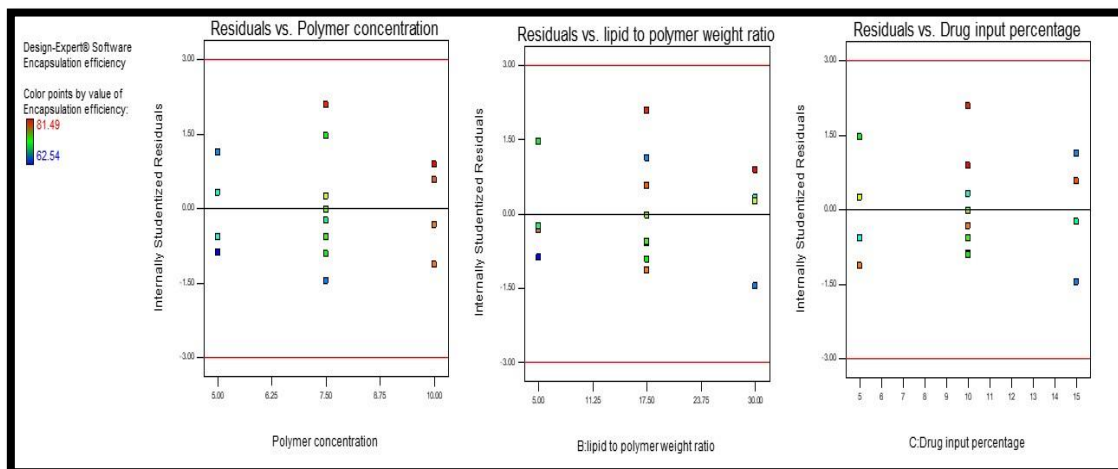


Figure 5-10 Residual vs. Individual factor plots

5.5.2.1.2.7 Piepel's plot

Piepel's plot is a trace plot showing the effect of individual factors plotting the pseudo limits of one component keeping the ratio of the changeable amounts of each component constant against the response. The responses are plotted as deviations from the reference blend i.e. centroid (pseudo center point of the constrained design). A steep slope for factor A (Concentration of polymer) and curvature for factor B and C (Lipid to polymer percentage ratio and Drug input percentage respectively) as shown in Figure 5-11 proves that the response is sensitive to factor. Hence line for the polymer concentration shows sharp steep which suggests that concentration of polymer has a great impact on the encapsulation efficiency.

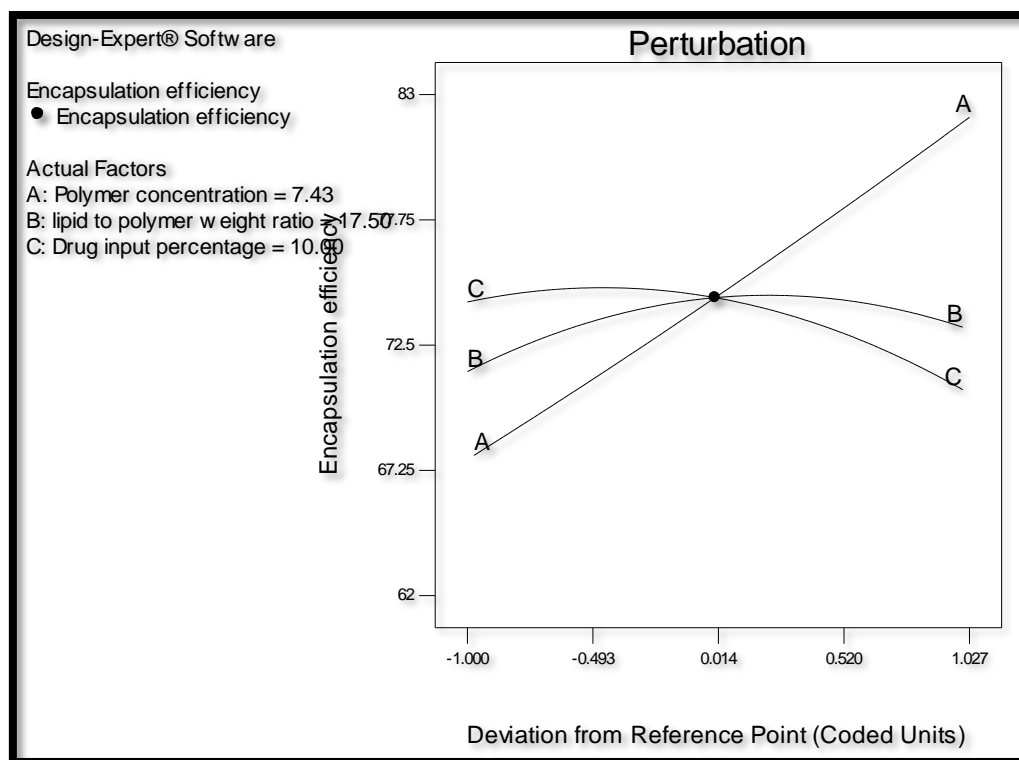


Figure 5-11 Piepel's plot

5.5.2.1.2.8 Response surface (3D) plots

The value of ANOVA gives us idea about the factors having significant effect on entrapment efficiency which is shown in contour and 3D plots. The RED area in the Figure 5-12 shows the area of maximum entrapment efficiency and BLUE zone represents the area with lowest entrapment efficiency.

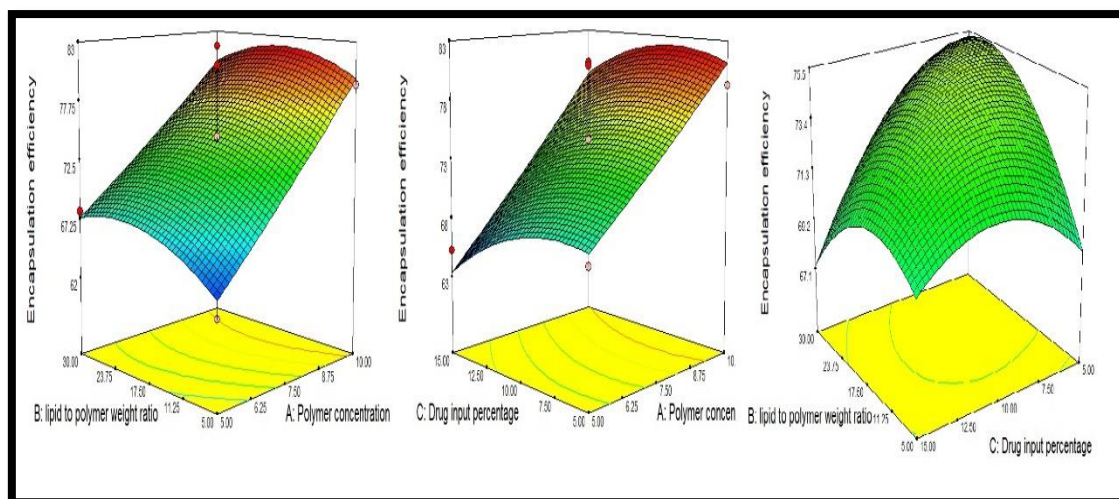


Figure 5-12 Effects of various factors on DTX entrapment by 3D surface curve

Two-factor 3D response surface plots for Docetaxel entrapment justifies the aforementioned significant terms. A quadratic model was found to have the best fit with the applied design and the higher cubic model was found to be aliased. From the plots it is concluded that increasing the concentration of Docetaxel and polymer initially increases the DTX entrapment but from a certain point the entrapment efficiency goes down. This may be due to limited loading capacity of Docetaxel in polymer matrix and lipid layer. All response surface (3D) shows combined effect of concentration of polymer, lipid to polymer percentage and drug input percentage on % entrapment efficiency. From the graph, increase in the entrapment efficiency were noticed with increasing concentration of polymer and lipid to polymer ratio. Though polymer concentration has great impact on the entrapment efficiency, there is some effect of outer lipid on the entrapment efficiency. The increment in Docetaxel entrapment efficiency is due to amphiphilic nature of block co-polymer PEG-PCL in which PCL chains confer hydrophobicity to PLHNCs and block co-polymer which can accommodate Docetaxel within its matrix inside PLHNCs. This result in agreement with Cryo-TEM reveals formation of multiple co-polymer amorphous unimers region in a frozen state with phase separated solid matrix core inside lipid bilayer. Polymeric core showed distinct PEG-PCL particles inside cavity of PLHNCs with embedded matrix formation.

5.5.2.1.3 Mathematical Model for Entrapment efficiency

Final equation in terms of coded factors has been obtained as below:

$$\text{Encapsulation efficiency} = +74.68 + 7.08 * A + 0.91 * B - 1.82 * C - 0.78 * A * B + 0.70 * A * C - 2.20 * B * C + 0.28 * A^2 - 2.17 * B^2 - 2.02 * C^2$$

5.5.2.2 Statistical analysis of response (dependent) variable 2: Particle size

5.5.2.2.1 ANOVA results of different models

Summary of the ANOVA results for different models as shown in Table 5-17 Summary of ANOVA results of different models for particle size which depicts sequential p-values and Lack of Fit p-values along with Adjusted and Predicted R-squared values for different models.

Table 5-17 Summary of ANOVA results of different models for particle size

Source	Sequential p-value	Lack of fit p-value	Adjusted R-squared	Predicted R-squared	Suggested model
Linear	0.9876	0.6421	0.8750	0.9332	
2FI	0.5058	0.8947	0.9822	0.9731	
Quadratic	<0.0001	0.8947	0.9829	0.9782	Suggested
Cubic	0.6421	-	0.9700	-	Aliased

Highest polynomial showing the lowest p value (<0.05) along with highest Lack of Fit p-value (>0.1) was considered for model selection. Based on the criteria quadratic model was found to be best fitted to the observed responses. Special cubic and higher models were not suitable for prediction either due to low R-squared values and/or due to higher p value as compared to quadratic model (As shown in Table 5-17). Quadratic and higher models were aliased indicating the confounding of the model terms when the other model implying that the predicted response would give the wrong idea of the actual response.

Table 5-18 ANOVA results of quadratic mixture model for particle size

Source	Sum of Squares	df	Mean Square	F Value	p-value Prob > F	
Model	497.21	9	55.25	4.93	<0.0001	significant
A-Polymer concentration	401.44	1	401.44	35.83	<0.0001	
B-lipid to polymer weight ratio	6.62	1	6.62	0.59	<0.0001	
C-Drug input percentage	26.46	1	26.46	2.36	0.3808	
AB	2.43	1	2.43	0.22	0.5891	
AC	1.95	1	1.95	0.17	0.2767	
BC	19.27	1	19.27	1.72	0.8008	
A²	0.34	1	0.34	0.030	0.7497	
B²	19.79	1	19.79	1.77	0.9234	
C²	17.18	1	17.18	1.53	0.9497	
Residual	78.42	7	11.20			
Lack of Fit	26.21	3	8.74	0.67	0.8947	not significant
Pure Error	52.21	4	13.05			

Cor Total		575.63	16			
ANOVA Summary						
Parameters	Results	Parameters	Results			
Std. Dev.	0.84	R-Squared	0.9891			
Mean	83.05	Adj R-Squared	0.9829			
C.V. %	1.01	Pred R-Squared	0.9782			
PRESS	30.10	Adeq Precision	29.663			

The ANOVA table revealed that the effect of factors was significant and hence the model is significant for the entrapment efficiency. The F value was highest for the factor A (401.44), i.e., increasing polymer concentration and would increase the particle size in linear manner. Polymer concentration and L/P ratio have most prominent effect as their p value is <0.0001. With increasing concentration of the polymer size of the polymeric core increased along with that increasing L/P ratio would give thickness to a lipid layer over the polymeric core which is responsible for additional increase in particle size. Other factors such as process parameters and drug input percentage (factor C) have low effect on particle size due to self-assembly of the system.

The Model F-value 4.93 suggests that the model is significant. There is only a 0.01% chance that a "Model F-Value" this large could occur due to noise. Values of "Prob > F" less than 0.0500 indicate model terms are significant. In this case A, B are significant model terms. Values of "Prob > F" greater than 0.1000 indicate the model terms are not significant. The "Lack of Fit F-value" of 0.67 implies the Lack of Fit is not significant relative to pure error. Non-significant lack of fit is good hence we want the model to fit. The "Pred R-Squared" of 0.9782 is in reasonable agreement with the "Adj R-Squared" of 0.9829. "Adeq Precision" measures the signal to noise ratio. A ratio greater than 4 is desirable. Our ratio of 29.663 indicates an adequate signal. This model can be used to navigate the design space.

5.5.2.2.2 Model diagnostic plots for encapsulation efficiency

5.5.2.2.2.1 Normal residuals plot

The normal probability plot (normal plot of residuals) which shows whether the residuals follows a normal distribution or not and helps to identify any specific patterns in the residual's indicative of requirement of transformations i.e. "S-shaped" curve, etc. Our normal plot of residuals for the current data follows a straight line, indicating no abnormalities. The data doesn't have to match up perfectly with the line. A good rule of thumb is called the "fat pencil" test. If you can put a fat pencil over the line and cover up all the data points, the data is sufficiently normal. In this case (As shown in Figure 5-13) the plot of residues falls near the

area of straight line (following fat pencil rule) hence proved that available data follows normal distribution and doesn't follow any specific pattern.

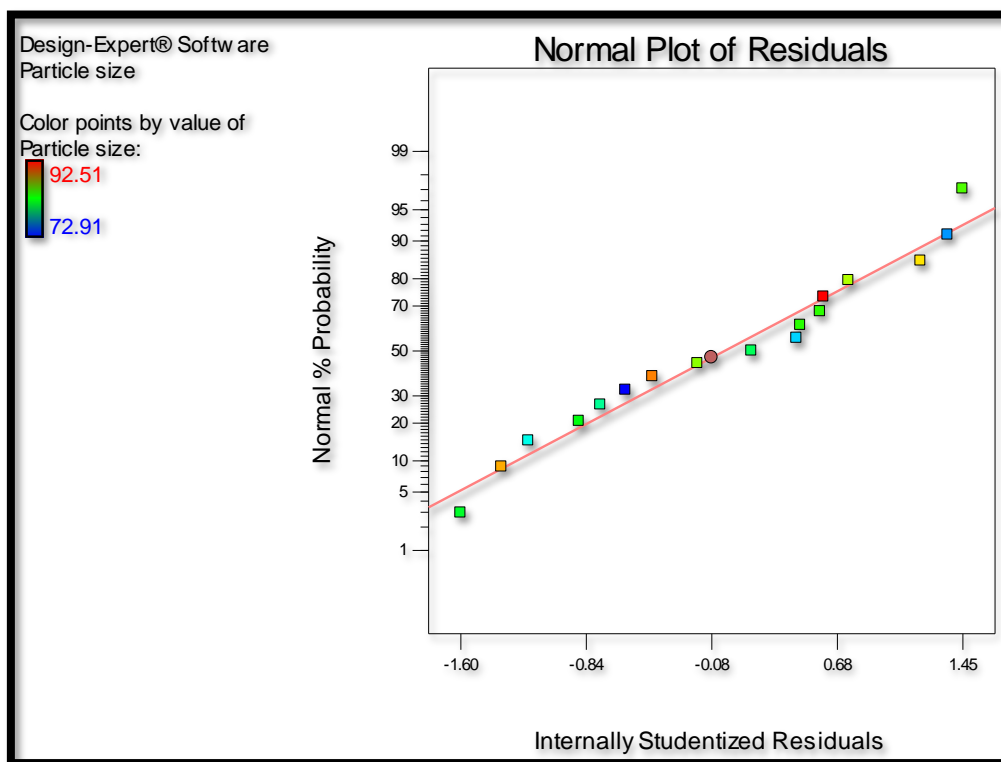


Figure 5-13 Normal plot of residuals for particle size

5.5.2.2.2 Residuals vs. predicted plot

Residuals vs. predicted response (ascending values) plot tests if variance is distributed over the design constantly i.e. variance is not associated with the factor values as megaphone patterns (pattern like horizontal cone sign $>$ or $<$) which indicate either decreasing or increasing residuals with increasing the factor values. This is a plot of the residuals versus the ascending predicted response values. The size of the residual should be independent of its predicted value. In other words, the vertical spread of the studentized residuals should be approximately the same across all levels of the predicted values. In this case (As shown in Figure 5-14) we didn't notice any horizontal cone shape in the plot from the current data hence the variance is distributed all over the design which proves that not a single variable has a predefined action on the particle size.

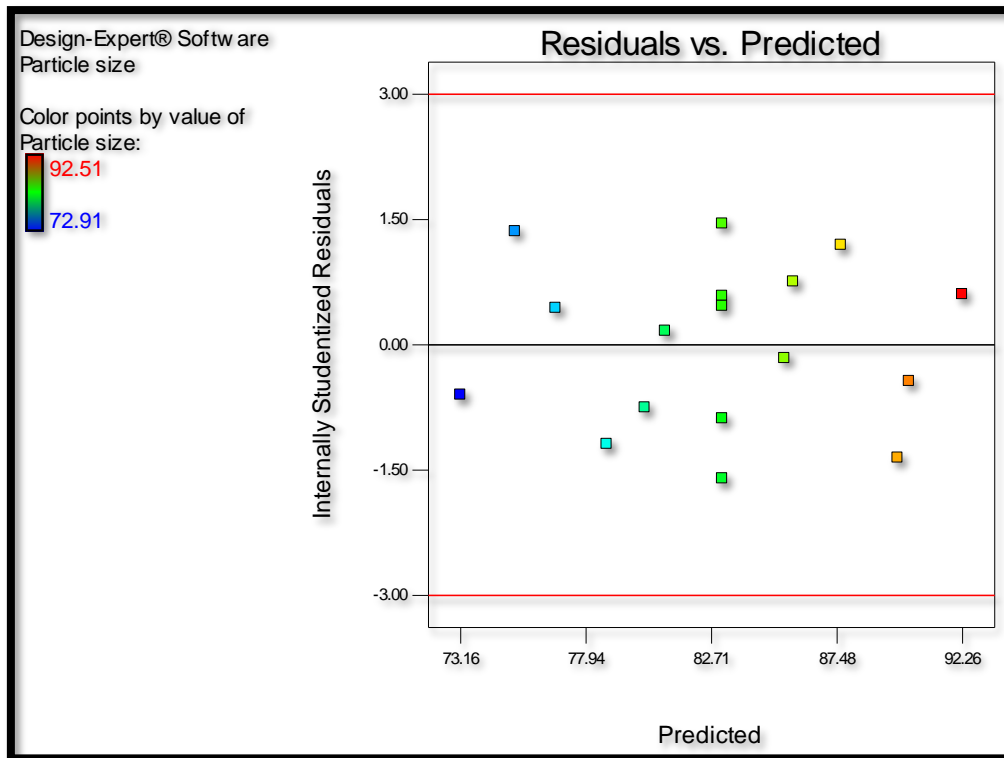


Figure 5-14 Residual vs. Predicted plot for particle size

5.5.2.2.3 Residual vs. Run plot

Residual vs. run order plots the residuals against the experimental run order i.e. order in which the experiments have been carried out. The current plot having a random scatter of residuals which indicate there is no time dependent change occurring in the residuals. In graph from Figure 5-15 there is no downward or upward trend noticed hence it is confirmed that experiment will be in random manner and selected model provide protection against any biased result in the design and point prediction.

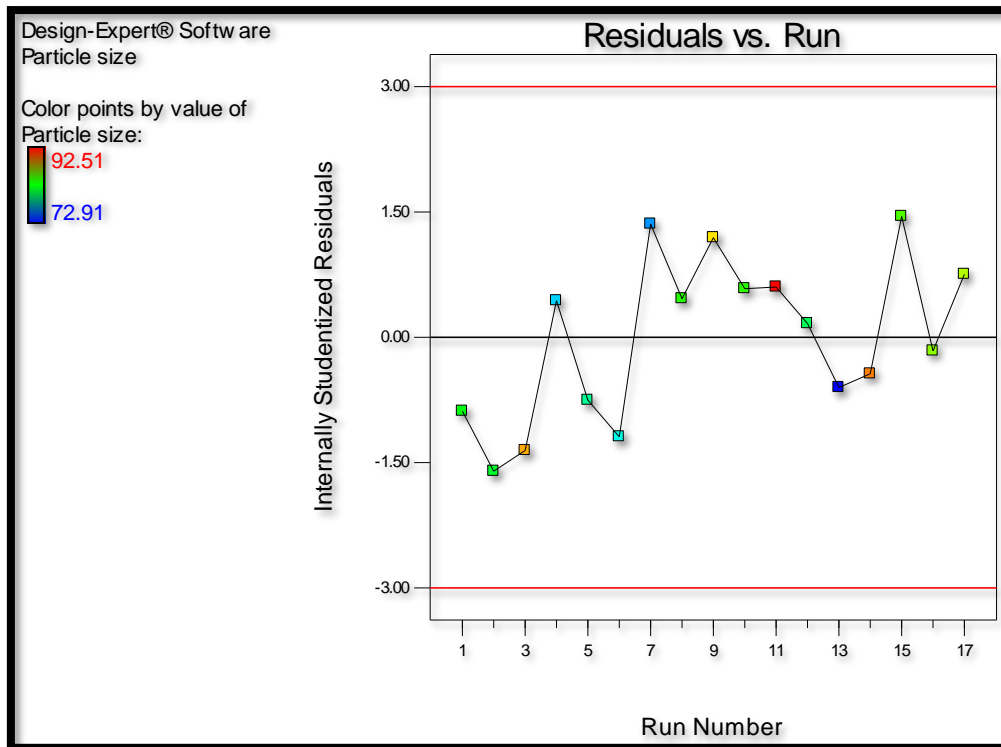


Figure 5-15 Residual vs. Run plot for particle size

5.5.2.2.4 Predicted vs. Actual plot

This plot shows correlation between the observed response values and actual response values. Hence plot from Figure 5-16 shows a straight line at 45° indicates that quadratic model which were selected to predict particle size on the basis of above mentioned three factors were appropriate over all the design matrix.

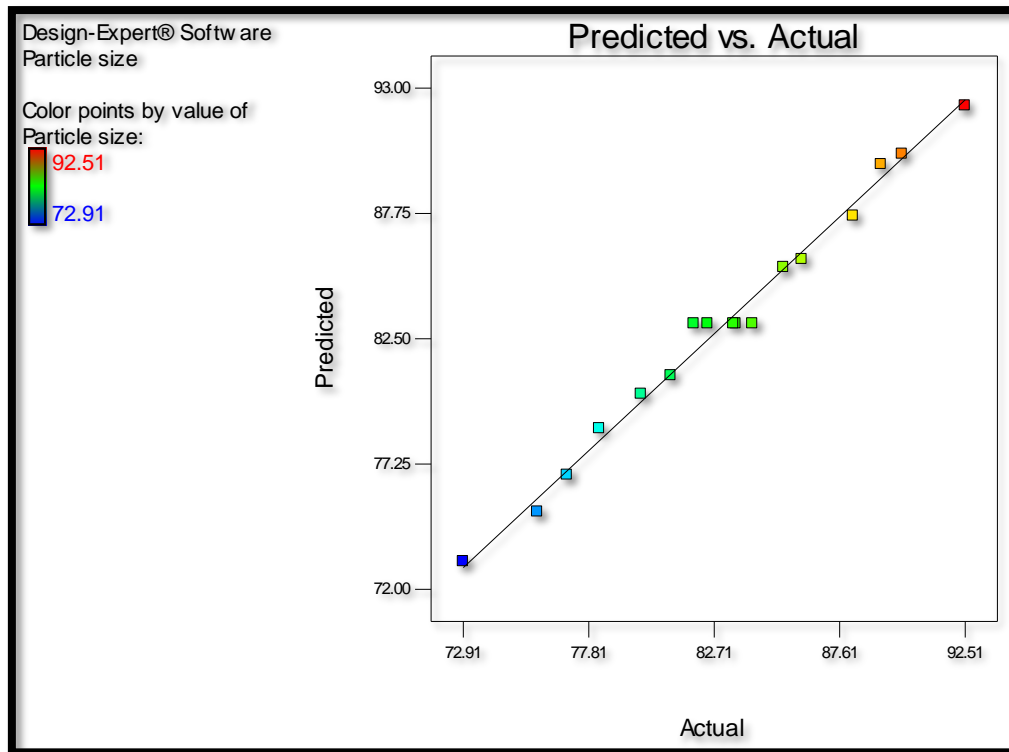


Figure 5-16 Predicted vs. Actual plot for the particle size

5.5.2.2.5 Box-cox plot for power transformation

Box-Cox plot of $\ln(\text{residuals sum of squares})$ vs. λ for power transformation helps select any power transformation of observed response values required for fitting the model based on the best λ value and 95% confidence interval around it. Plot in Figure 5-17 shows the λ value of 1, which lies near the best λ value and within 95% confidence interval of it, indicating no requirement for any power transformation.

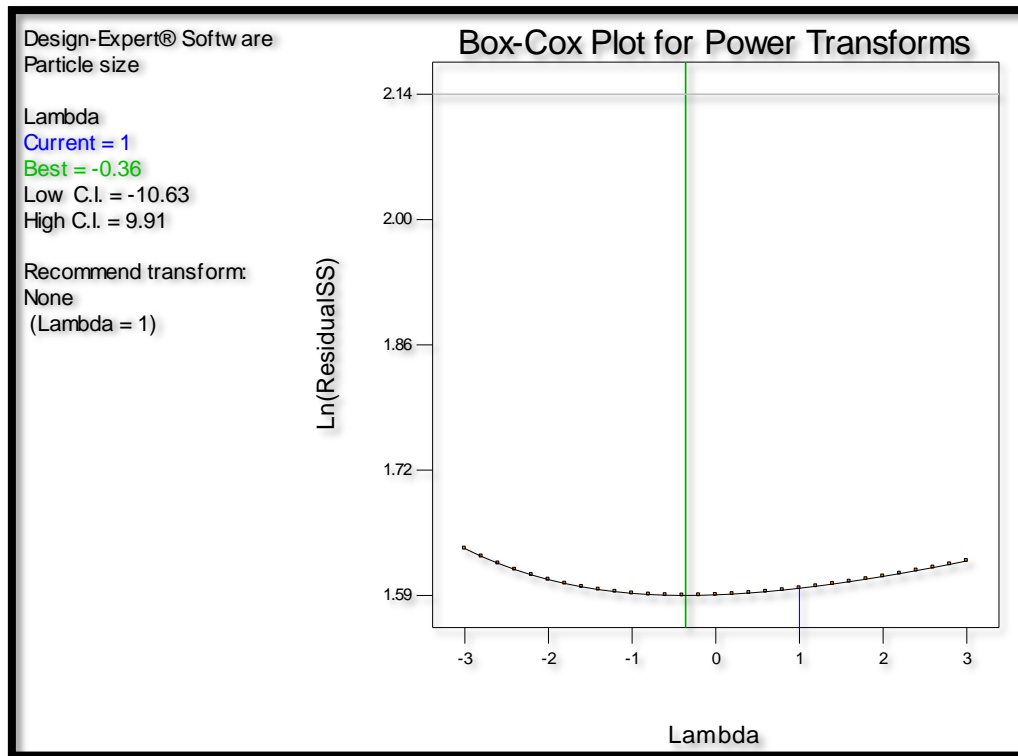


Figure 5-17 Box-Cox plot for Power transformation for the particle size

5.5.2.2.6 Residual vs. Factor plots

Plot of residuals vs. any factor evaluated if any association is there between the variance associated with different levels of factor i.e., any specific trends (+ve or -ve curvatures) associated with increasing level of each factor. As it can be seen from the Figure 5-18 plots for each factor shows a random scatter which indicates that model is effective in accounting for the variance of individual factor.

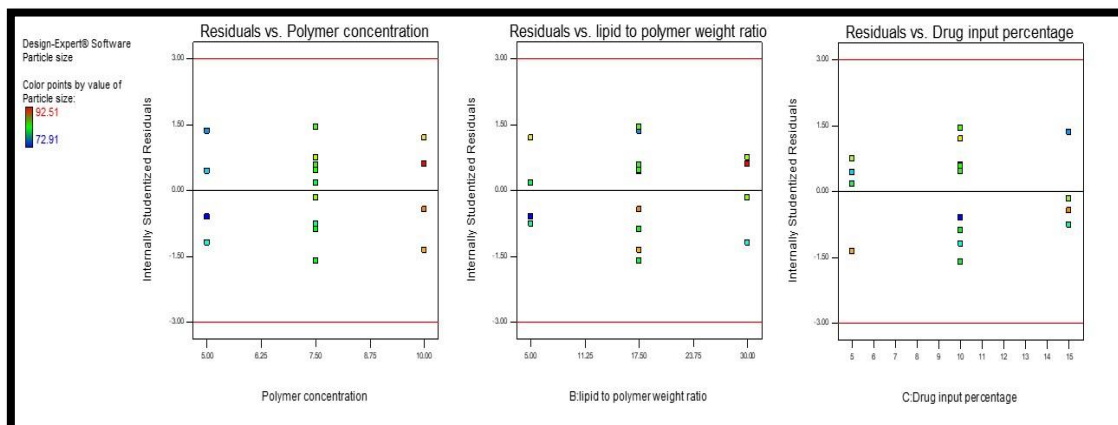


Figure 5-18 Residual vs. Individual factor plots

5.5.2.2.7 Piepel's plot

A steep slope for factor A (Concentration of polymer) and factor B (Lipid to polymer percentage ratio) shows a huge impact of both factors on the particle size of PLHNCs. Whether line for the factor C (Drug input percentage) is straight horizontal compare to other factors which shows low impact of drug input percentage on the particle size.

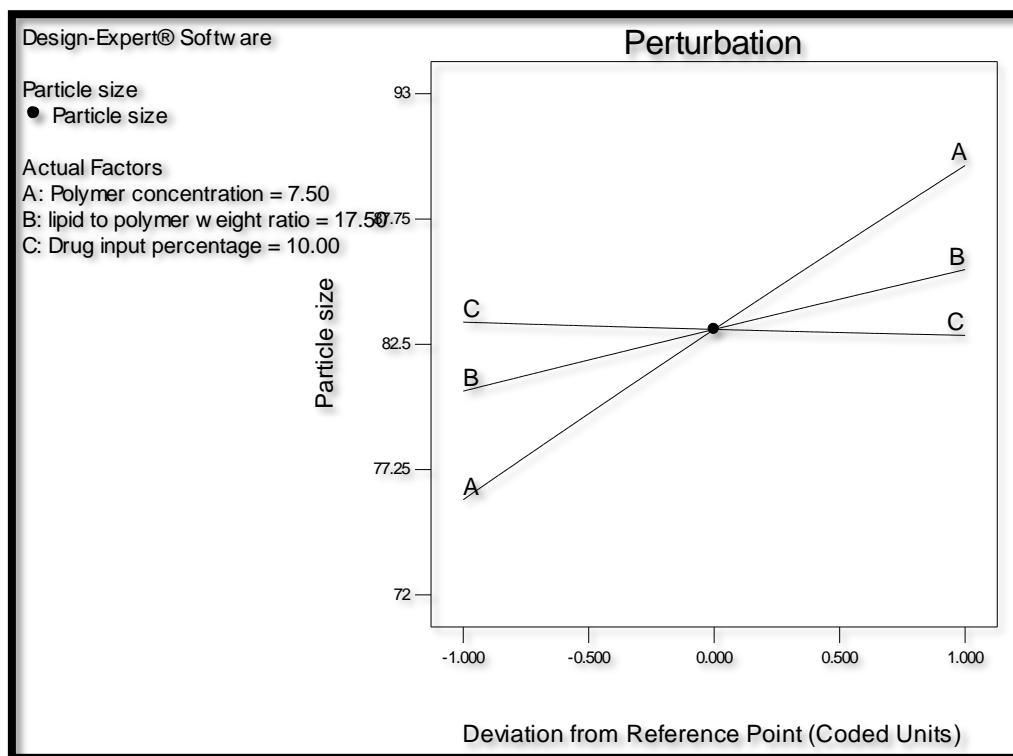


Figure 5-19 Piepel's plot for particle size

5.5.2.2.8 Response surface (3D) plots

The value of ANOVA gives us idea about the factors having significant effect on particle size which is shown in contour and 3D plots. The RED area in the Figure 5-20 shows the area of maximum size and BLUE zone represents the area with lowest size.

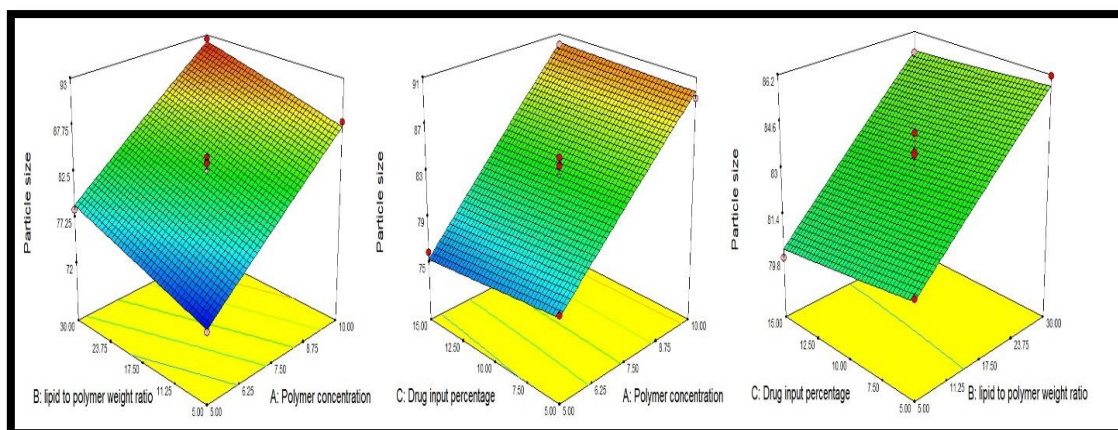


Figure 5-20 Effects of various factors on PLHNCs particle size by 3D surface curve

Two-factor 3D response surface plots for particle size of PLHNCs justifies the aforementioned significant terms. All response surface (3D) which shows combined effect of concentration of polymer, lipid to polymer percentage and drug input percentage on particle size of PLHNCs. From the Response surface (3D) shows combined effect of polymer concentration and lipid to polymer weight ratio on PLHNCs size. It has been concluded that as there is increase in polymer concentration there is no significant change increase in nanocarriers size which was further confirmed from the ANOVA data as the P-value for Factor –A (i.e polymer concentration) was < 0.05 which suggest this factor is significant for nanocarrier size. In case of Factor B (i.e. lipid to polymer percentage) the P-value was < 0.05 which suggest that factor B is significant to nanocarrier size. From the plots it is concluded that increasing the concentration of polymer and lipid initially increases the DTX entrapment but from a certain point effect on particle size remains stable. This may be due to self-assembly of the particle during the formulation preparation which increases the number of particles in the formulation rather than forming big size particle once the CMC (critical micelle concentration) of the lipid is achieved.

5.5.2.2.3 Mathematical model for particle size

Final equation in terms of coded factors has been obtained as below:

$$\text{Particle size} = +83.12 + 7.00 * A + 2.55 * B - 0.28 * C - 0.24 * A * B + 0.49 * A * C + 0.11 * B * C - 0.14 * A^2 - 0.041 * B^2 + 0.027 * C^2$$

5.5.3 Desirability plot and overlay plot for optimization

A desirability plot gives optimum value of variables so as to be obtained desired responses. Desirability plot was generated using Design Expert 7.0.0. Parameters for the desirability batch are shown in Table 5-19.

Table 5-19 Variables for desirability plot and goals for response

Name	Goal	Limit	Limit
A. Polymer Concentration (mg/ml)	In range	5.0	10.0
B. Lipid to polymer percentage	In range	5.0	30.0
C. Drug input percentage	In range	5.0	15.0
Quality target			
Nanocarrier size (nm)	Minimum	72.91	92.51
Entrapment Efficiency	Maximize	62.54	81.49

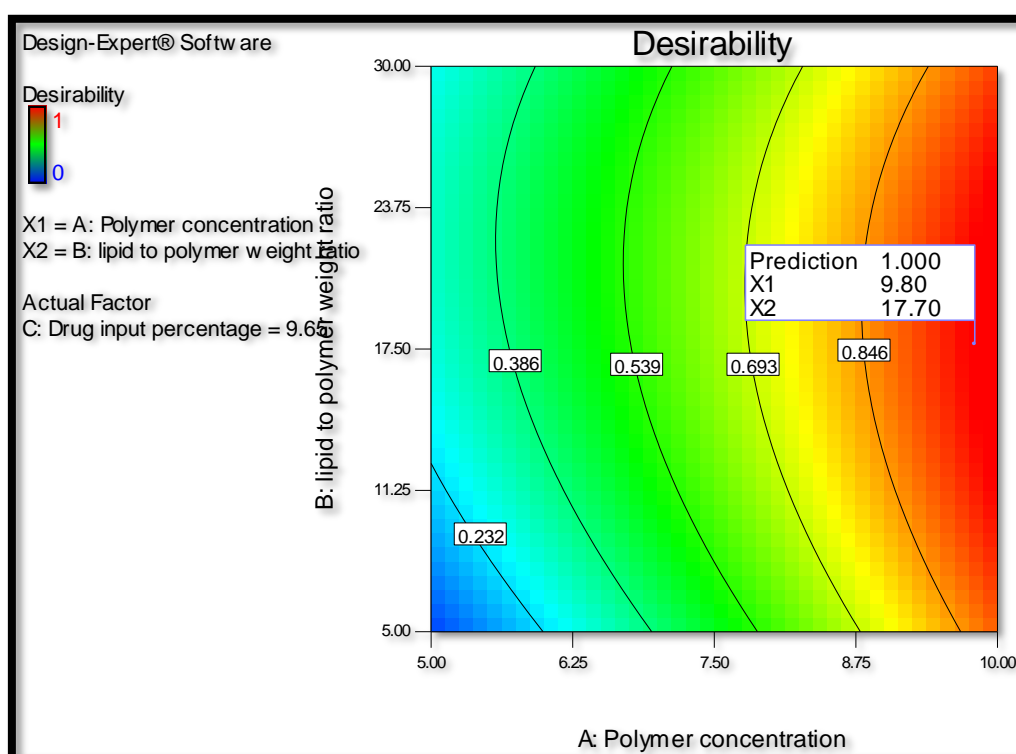


Figure 5-21 Desirability plot

5.5.4 Point prediction and confirmation

From the Box-Behnken design, two most desirable batches were selected for further optimization of lyophilization and dry powder formulation on the applied constraint. Confirmation of responses was done by carrying out the experiment using the selected factor values in triplicate. (Shown in Table 5-20)

Table 5-20 Experimental validation of predicted optimized batch

Variables	Goal	Lower Limit	Upper Limit	Predicted batch of PLHNC 1	Actual batch of PLHNC 1	Predicted batch of PLHNC 2	Actual batch of PLHNC 2
Optimization of Docetaxel PLHNCs							
A: Polymer concentration (mg/mL)	in range	5	10	10.0	10.0	10.0	10.0
B: L/P percentage ratio (%)	in range	5	30	29.58	30.00	25.26	25.00
C: Drug input (%)	in range	5	15	6.54	7.00	5.03	5.00
Docetaxel Entrapment (%)	maximize	62.54	81.49	81.49	85.6 ± 2.8	81.56	91.5 ± 1.4
Particle Size (nm)	minimize	72.91	92.51	91.92	124.1 ± 1.9	91.36	126.3 ± 1.6
Zeta potential					26.5 ± 1.8		22.4 ± 1.4
PDI					0.121 ± 0.12		0.108 ± 0.11
% Complexation of shRNA pDNA					97.4 ± 1.6		96.9 ± 1.8

5.6 CHARACTERIZATION

5.6.1 Particle size and zeta potential determination

The particle size of PLHNCs was determined under the principle of dynamic light scattering using Malvern Zetasizer Nano (Nano ZS, Malvern Instruments, UK). The light source was 633 nm He-Ne laser and the scattering angle was 175°. Analyses were carried out at 25 °C temperature after diluting 0.2 mL of formulation to 2 mL using filtered (filtered with 0.22µm nylon membrane filter) double distilled water. The total number of sub-runs for the size measurement were 15 and each run was for a duration of 10 seconds. The results were

reported as Z-average. Zeta potential of the developed PLHNCs was determined using the same instrument as per Smoluchowski's equation from the electrophoretic mobility of the sample at 25 °C.

5.6.2 Determination of encapsulation efficiency of Docetaxel and complexation efficiency of shRNA

The exact amount of Docetaxel incorporated in PLHNCs was identified by the RP-HPLC method. Extraction of Docetaxel from PLHNCs was successfully performed before injection. Each mL of PLHNCs suspension was diluted with tertiary butyl methyl ether to make the final volume of 5 mL. Above mixture was then vortexed for 30 sec to achieve homogeneity. Subsequently, the vortexed mixture was subjected to centrifugation at 10,000 rpm for 10 mins to separate organic layer from the aqueous one. The organic layer was then transferred to a separate vial and subjected to nitrogen drying. Residues of the drying were then reconstituted with 100 µL of the mobile phase (acetonitrile:water). From that, 20 µL of sample was injected into the RP-HPLC system. Estimation of docetaxel content in PLHNCs was performed by reverse-phase HPLC method/RP-HPLC (Agilent Technologies 1260 infinity II) using C18 ODS (octadecyl silane) column (250 mm * 4.6 mm * 5 µm, Thermo scientific) at ambient temperature. The mobile phase acetonitrile: water (60:40) was allowed to run at a flow rate of 1 mL/min. Estimation of Docetaxel was examined using a UV-visible detector at a wavelength of 231 nm.

$$\% \text{ entrapment efficiency} = \frac{\text{Amount of drug entrapped}}{\text{Total amount of drug}} \times 100$$

Complexation of ABCB1 shRNA plasmid with the PLHNCs was evaluated by centrifugation and UV analysis using NanoDrop 1000 (ThermoScientific, USA). ABCB1 shRNA plasmid and Docetaxel loaded PLHNCs were centrifuged at 18000 rpm for 2 h at 4°C (Remi centrifuge, Remi, USA) to settle down the PLHNCs. Then, the supernatant was analyzed on the NanoDrop 1000 and the content of pDNA was calculated using the standard expression OD1 = 50 µg/mL of double-stranded pDNA. Readings from formulations were compared to those from standard dilution of naked ABCB1 shRNA plasmid. Complexation efficiency was calculated using the following equation;

% Complexation efficiency

$$= \frac{(\text{Absorbance}_{\text{naked ABCB1 shRNA standard}} - \text{Absorbance}_{\text{supernatant}})}{\text{Absorbance}_{\text{naked ABCB1 shRNA standard}}} \times 100$$

5.6.3 Phospholipid content by Stewart method

Total Phospholipid content was measured in the PLHNCs formulation. 2ml PLHNCs formulation was taken and procedure mentioned in chapter 3 was performed.

5.6.4 Scanning Electron Microscopy (SEM) Analysis

SEM was conducted using EVO-18 ZEISS at the Department of Metallurgy, Maharaja Sayajirao Rao University of Baroda, to determine particle morphology. For PLHNCs, SEM analysis was conducted by drying and immediately observing the dispersion of PLHNCs on the grid.

5.6.5 Transmission Electron Microscopy (TEM)

TEM analyses were carried at an acceleration voltage of 200 kV on a Technai, Phillips Holland, at the Sophisticated Instrumentation Center for Applied Research and Testing (SICART) Vallabh Vidyanagar instrument. By administering the PLHNCs onto a 300-mesh Formvar-coated copper grid (previously hydrophilized under UV light), the TEM sample was prepared (Electron Microscopy Sciences, Hatfield, PA). After 30 min of incubation, samples were blotted away and grids were negatively stained at room temperature for 10 min with 2 percent (w/v) uranyl acetate aqueous solution freshly formulated and sterile-filtered. The grids were double washed with purified water and air dried until imaging.

5.6.6 In-vitro drug release study and drug release kinetics

Solutions:

- **Sodium Sulphide solution 0.3%:** 0.3 g of accurately weighed sodium sulphide was dissolved in 100 ml distilled water to produce 0.3% Sodium Sulphide solution.
- **Sulphuric acid solution 0.2%:** 0.2 mL of concentrated sulphuric acid was dissolved in 100 mL of distilled water to produce 0.2 % sulphuric acid solution.
- **Potassium Dihydrogen Phosphate, 0.2M :**27.218 g of potassium dihydrogen phosphate was dissolved in 1000 mL of distilled water to produce 0.2M Potassium Dihydrogen Phosphate solution.
- **Sodium Hydroxide, 0.2M:** 8.0 g of sodium hydroxide was dissolved in 1000 mL of distilled water to produce 0.2M Sodium Hydroxide solution.
- **Phosphate Buffer:** 50.0 mL of the 0.2M potassium dihydrogen phosphate, 0.2M was taken in a 200-mL volumetric flask and specified volume of 0.2M sodium hydroxide, 0.2M and then water was added to make the final volume up to 200-mL. The pH of the

buffer was checked using pH meter and adjusted if needed using sodium hydroxide solution or hydrochloric acid solution as necessary.

- **Amount of 0.2M NaOH to be added to 0.2M KH₂PO₄ Solution to get Buffer of Required pH**

Table 5-21 Amount of 0.2 M NaOH required

pH	0.2 M NaOH (mL)
6.6	16.4
7.4	39.1

- **Acetic acid solution 2N(18):** 116 mL of glacial acetic acid was dissolved in sufficient quantity of distilled water and after cooling of solution to room temperature final volume was made upto 1000 mL.
- **Acetate Buffer pH 5.5 (18):** 5.98 g of sodium acetate trihydrate was weighed and sampled in a 1000 mL volumetric flask. To this 3.0 mL of the acetic acid solution was added and volume was made up to 1000 mL. The pH of the buffer was checked using pH meter and adjusted if needed using acetic acid solution or sodium hydroxide solution as necessary.

Dialysis membrane Set-Up/activation

Before using dialysis membrane in drug release study it should be activated by below mentioned process.

1. The 5 cm long dialysis membrane was cut and kept for 3 hours in running water for glycerin elimination.
2. After that the dialysis membrane was dipped in 0.3 percent w/v solution of sodium sulphide solution for 1 min at 80°C.
3. The dialysis membrane treated with sodium sulphide was then dipped at 60° C for 1 min in warm water to extract sodium sulphide.
4. The dialysis membrane was then soaked in 0.2% H₂SO₄ for 1 min.
5. Then it was dipped again in the warm water for H₂SO₄ elimination.
6. This activated dialysis membrane was then kept in Phosphate buffer (pH 7.4) for 24 h prior to drug release studies.

PLHNCs containing shRNA pDNA were suspended in TE buffer pH 7.4 (1 ml) and incubated at 37°C on a shaker at 100 r.p.m. At different time-points, the buffer was separated from the NP by centrifugation at 20,000 r.p.m. for 10 min and analysed for the amount and integrity of released pDNA (8). Then, the supernatant was analysed on the NanoDrop 1000 and the content

of pDNA was calculated using the standard expression $OD1 = 50 \mu\text{g/mL}$ of double-stranded pDNA.

To simulate the physiological environment of tumor cells, interstitium of tumors and blood or normal cell, phosphate buffer with pH 5.5, 6.6, and 7.4 were investigated for in-vitro drug release study (9). A drug release study was performed using a dialysis bag with molecular mass cutoff of 3000 Da for 72 h. 2 mL of the formulation was filled in a dialysis bag and dipped in receptor media comprising 200 mL phosphate buffer at 37 °C. At 1, 2, 4, 8, 12, 24, 48, 72 h, 1 mL of sample was withdrawn periodically and fresh media was replaced to maintain sink condition. These samples were analysed using HPLC and the % Docetaxel and shRNA pDNA released was calculated and plotted against the time to obtain the release curve. Data of drug release are fitted in zero order, first order, Higuchi, Korsmeyer–Peppas and Hixon-crowell models to determine release kinetic pattern from PLHNCs (10, 11).

1. Zero order release

For Docetaxel and shRNA pDNA release that follows zero order kinetics following equation can be applied

$$M_t = kt$$

Where, M_t = amount of drug or pDNA released at time t

k = zero order release rate constant

t = time

2. First order release

For Docetaxel and shRNA pDNA that follows first order kinetics following equation can be applied

$$\ln[1-(M_t/M_0)] = -kt$$

Where, M_t = amount of drug or pDNA released at time t

M_0 = initial amount of drug or pDNA present

k = first order release rate constant

t = time

3. Higuchi's model

Following equation can be applied for Docetaxel and shRNA pDNA release that follows Higuchi's kinetics model.

$$M_t = kt^{1/2}$$

Where, M_t = amount of drug or pDNA release at time t

k = Higuchi's release rate constant

t = time

4. Korsmeyer –Peppas model

Following equation can be applied for Docetaxel and shRNA pDNA release that follows Korsmeyer –Peppas kinetics model.

$$\ln M_t/M_0 = \ln k + n \ln t$$

Where, M_t = amount of drug or pDNA released at time t

M_0 = initial amount of drug or pDNA present

k = Korsmeyer –Peppas release rate constant

t = time

n = Diffusional exponent that characterizes the mechanism of drug release.

The value of diffusional exponent 'n' will help to understand mechanism of drug release from dosage forms of different geometry like slab, cylinder, sphere etc.

- n = 0.5 to 1 (0.5 < n < 1) indicates non Fickian release
- n = 0.5 indicates Higuchi's Kinetics
- n = 1 indicates the first order release or case 2 transport.
- n < 0.5 indicates Fickian release.
- n > 1 indicates the Super case 2 transport.

5. Hixon Crowell model

Following equation can be applied for Docetaxel and shRNA pDNA release that follows Hixon Crowell kinetics model.

$$\sqrt[3]{M_0} - \sqrt[3]{M_t} = kt$$

Where, M_t = amount of drug or pDNA released at time t

M_0 = initial amount of drug or pDNA present

k = Hixon Crowell release rate constant; t = time .

5.6.7 Estimation of residual solvent by Head space gas chromatography

Standard Preparation: The typical acetonitrile assay was carried out by taking 100µl of acetonitrile in a 10 ml volumetric flask and adjusting the level with DMF so that the final concentration will be 10,000 ppm. Take 1 ml in a 10 ml volumetric flask from the above solution and deionized water was used to make up the mark, so the concentration was 1000 ppm.

Sample Preparation: 100µl of PLHNCs formulation was taken in 10 ml volumetric flask and diluted up to mark using DMF. From the above solution, 1ml was taken and added to 5ml volumetric flask to make up the volume using Deionized water (12).

5.6.8 Atomic force microscopy (AFM) analysis

AFM was performed using AFM-NT-MDT (Model No. NT-MDT NTEGRA Prima) using silver nitride cantilever at Indian Institute of Technology, Gandhinagar. AFM images were captured for PLHNCs using the NT-MDT NTEGRA Prima Scanning Probe Microscope (SPM) in tapping mode using the tapping mode 100 μ X 100 μ scanner and the edge-sized NSG tip about 10 nm at an intensity of 1.01 Hz. Silicon wafer, Si (100) with an overall root mean square roughness (RMS) of 0.065 for bare interfaces was the standard substrate used for the analysis. On the Si (100) substrate, a drop of dilute solution of NPs was deposited, which was dried under atmospheric conditions for 24 hours. The covered substratum region was subjected to SPM scans of 10 μ x 10 μ and 5 μ X 5 μ . With Nova software supplied with the tool, the topography image was made. Average roughness analysis and distribution of particle size were analyzed in the scanned region. The atomic force microscope (AFM) method has become a valuable instrument for direct measurements of microstructural parameters and for unraveling intermolecular forces with atomic-resolution characterization at the nanoscale level.

5.7 RESULTS AND DISCUSSION

5.7.1 Particle size analysis of PLHNCs by dynamic light scattering (DLS)

Drug-loaded PLHNCs must have a small size distribution of the mean sub-micrometer, along with a biocompatible zeta potential and an appropriate drug loading in order to provide therapeutic benefits as a drug delivery system. The nanocarrier size obtained in the present study (As shown in Figure 5-22) was between 123.9 and 128.6 nm, with a very fine polydispersity index of 0.0988 and 0.124 nm for PLHNC1 and PLHNC2 respectively.

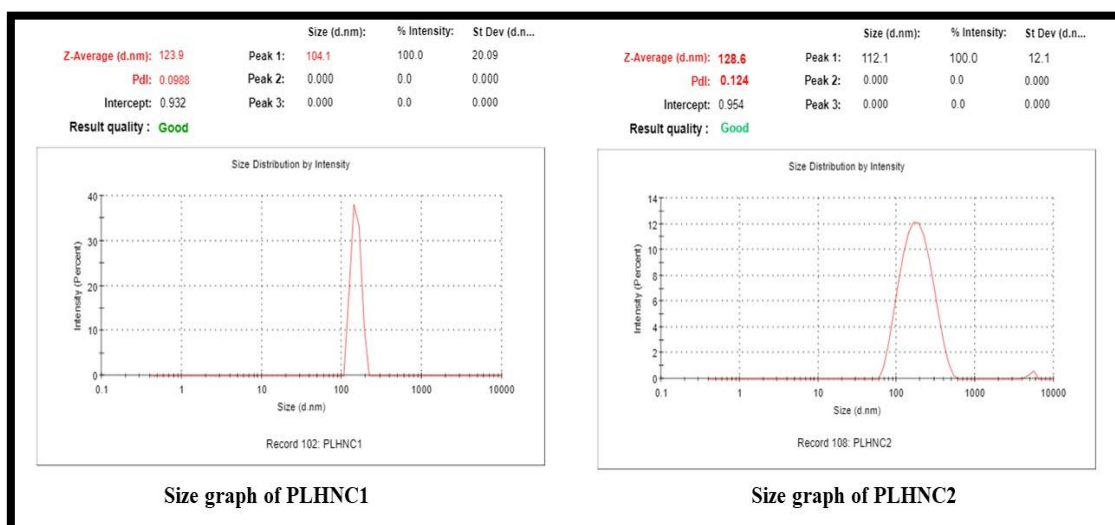


Figure 5-22 Size and PDI of optimized PLHNCs batch

Nanocarrier Size was significant property of PLHNCs, as it can affect the biopharmaceutical properties of the PLHNCs. The biodistribution of particulate matter can also depend on the size of the particle and particle endocytosis is also dependent on size. Another size-dependent phenomenon was stated to be particle uptake, where the small particles could be picked up effectively relative to the larger particles. Particle size is important for cancer cells to target the EPR (Enhanced Permeability and Retention) effect, which plays a very critical role in targeting.

5.7.2 Zeta potential of developed PLHNCs

The zeta potential of PLHNCs were found to be $+28.18\text{mV} \pm 1.63$ and $+22.6\text{mV} \pm 1.14$ which has been shown in

Figure 5-23 Positive zeta potential of PLHNCs were due to presence of cationic lipid on outer lipid layer i.e., DOTAP. Positively charged PLHNCs particle will repel each other and account for stability by preventing aggregation. Moreover, Cationic charge of PLHNCs is advisable for the higher shRNA pDNA complexation and even for higher cellular uptake.

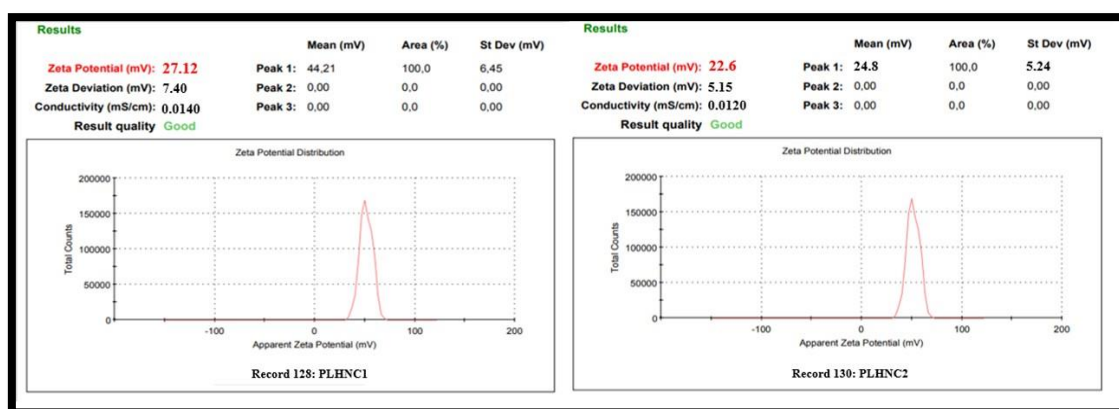


Figure 5-23 Zeta potential of optimized PLHNCs batch

5.7.3 Estimation of total phospholipid content

The amount of phospholipid determined by Stewart method has been found similar to the calculated phospholipid content of PLHNC1 and PLHNC2. Which suggest that there was no reaction between phosphate group of lipids in the formulation, and lipid layer remained intact on the surface of polymeric core.

Table 5-22 Total phospholipid content present in optimized batch

PLHNC batch	Calculated amount of phospholipid	Obtained amount of phospholipid
PLHNC1	2.5 mg/ml	2.34 ± 1.67
PLHNC2	3.0 mg/ml	2.98 ± 1.45

5.7.4 Scanning Electron Microscopy (SEM) Analysis

Vesicle structure were confirmed with surface visualization and circular shapes with a scale of approximately 170 nm were observed as shown in Figure 5-24.

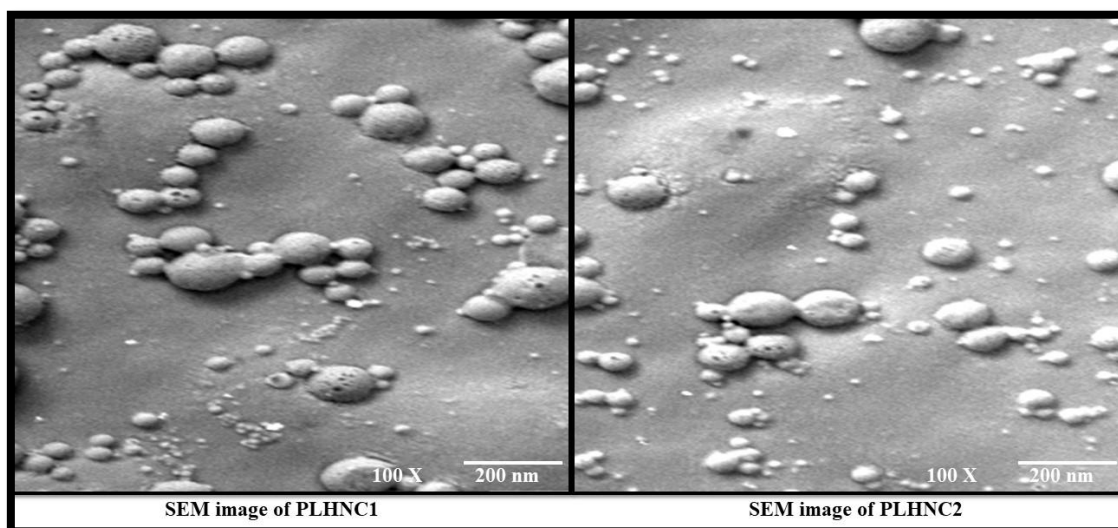


Figure 5-24 SEM images of optimized batch of PLHNCs

5.7.5 Transmission Electron Microscopy (TEM)

Negative staining with uranyl acetate in TEM was conducted for structural characterization of PLHNCs, which stains the lipid layer that was observed as a dim ring circling the polymeric centre (as shown in

Figure 5-25). The ring diameter is less than 20 nm which confirms the morphology and architecture of PLHNCs, i.e., the formation inside the lipid bilayer of several co-polymer amorphous unimers area in a frozen state of phase segregated stable matrix centre. With embedded matrix forming, the polymeric centre showed separate PEG-PCL particles inside the PLHNC cavity as well as reinforcing the PLHNC architecture relative to liposomes alone.

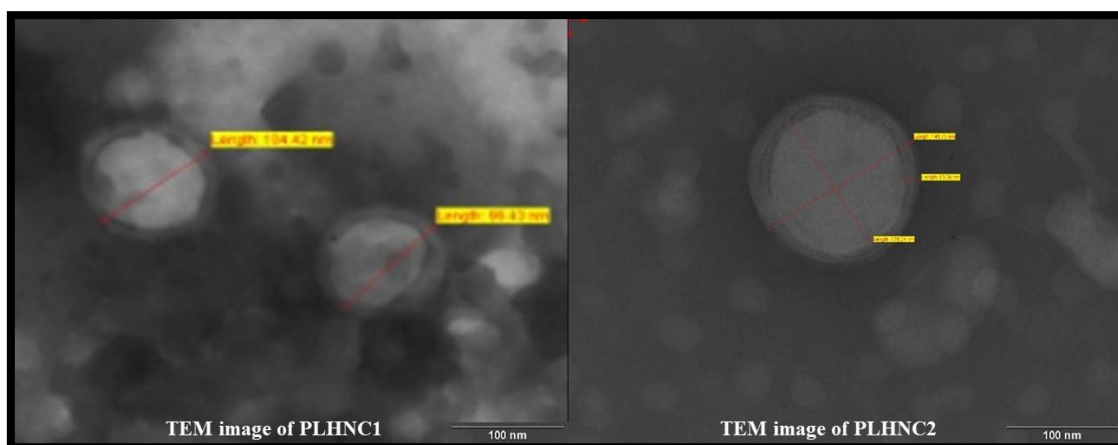


Figure 5-25 TEM images of optimized batch of PLHNCs

5.7.6 In-vitro drug and pDNA release study and release kinetic

Docetaxel loaded PLHNCs have followed the sustained release kinetics (As shown in **Figure 5-26**). From the three-release condition, the highest sustained-release curves have been obtained in receptor media of pH 5.5, which suggested the maximum sustained release of the drug in the cancer cells (13). Release of the docetaxel from the PLHNCs in the different media was observed to be in decreasing order, pH 5.5 > pH 6.6 > pH 7.4, which supports least docetaxel release in plasma and blood. The initial pattern of the burst release was found at pH 5.5 and pH 6.6, which can be due to sudden diffusion of the docetaxel present either on the surface or just beneath the lipid layer in the PLHNCs. The later sustained release pattern was achieved owing to the presence of drug in the core of PEG-PCL diblock copolymer.

Release of shRNA pDNA from PLHNCs also followed sustained release profile as shown in Figure 5-27. Cationic lipid in the formulation is responsible to hold the negatively charged shRNA pDNA molecule for the longer period.

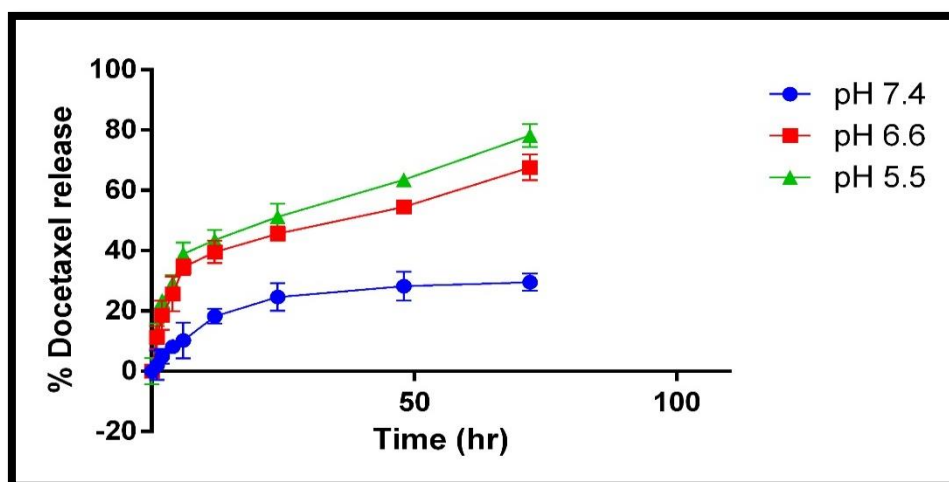


Figure 5-26 Docetaxel drug release pattern in different release media

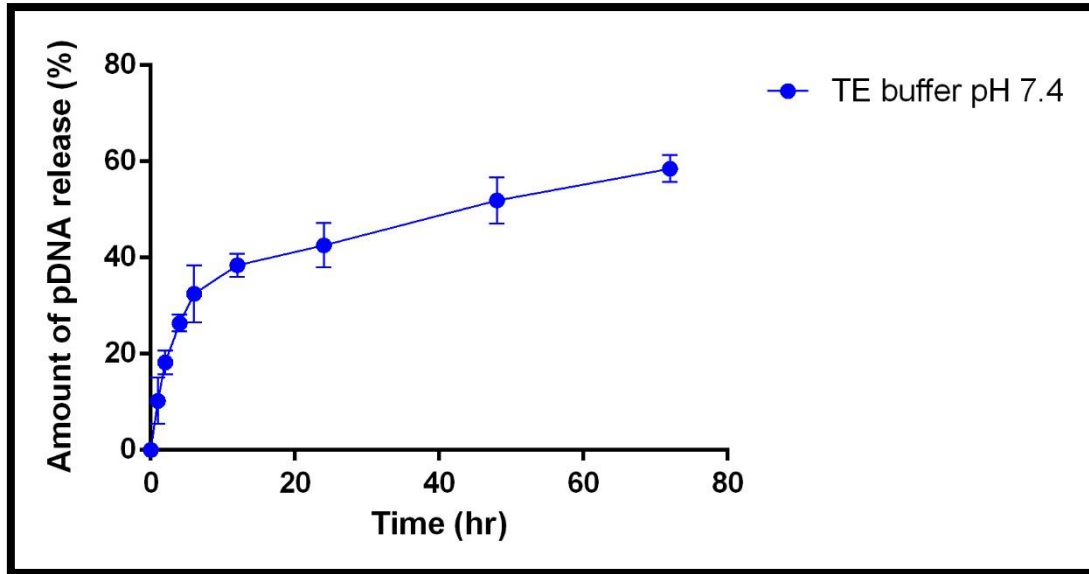


Figure 5-27 Release of shRNA pDNA from PLHNCs

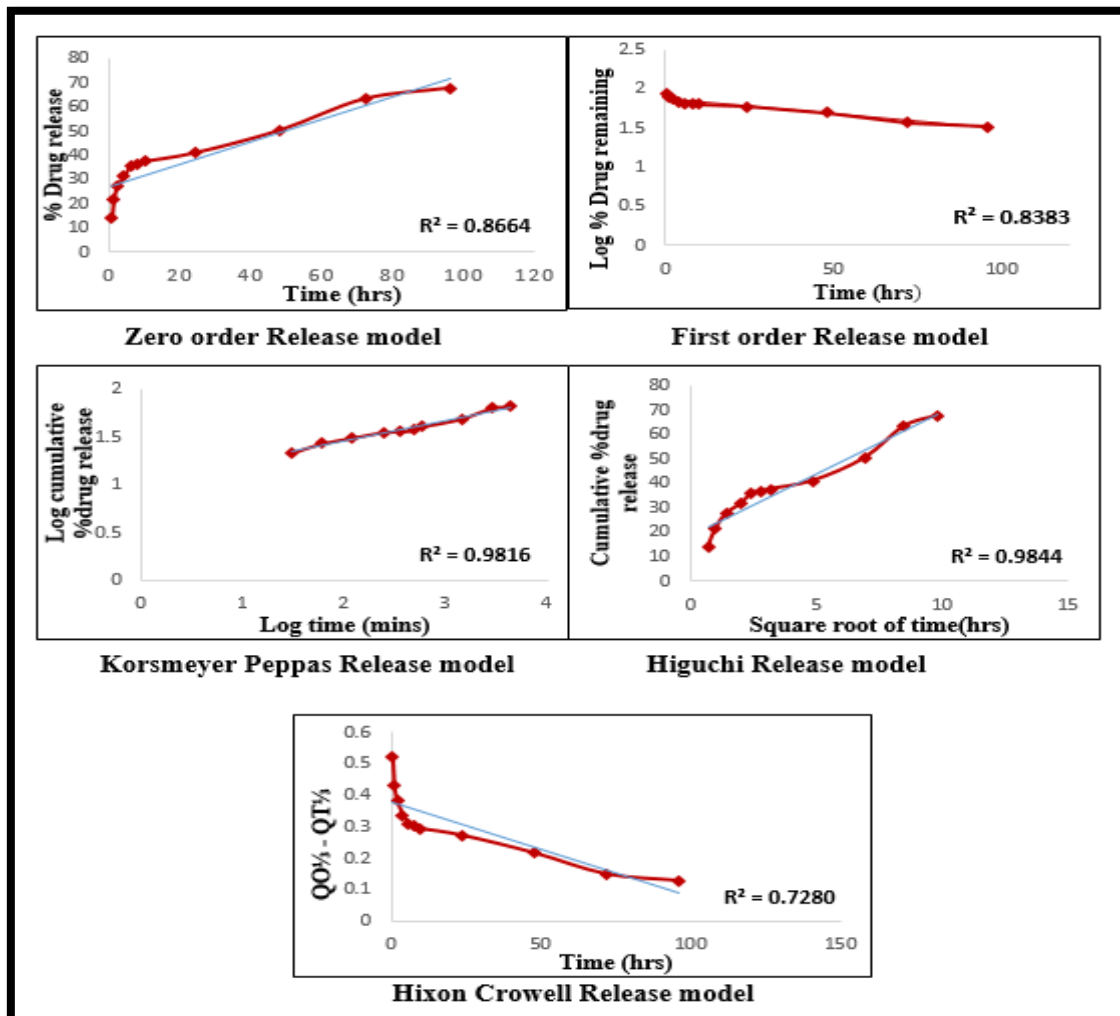


Figure 5-28 In-Vitro Release model of Docetaxel

From the kinetic model fitting analysis, it was concluded that for Docetaxel loaded PLHNCs the best fit was Higuchi model (As shown in Figure 5-28) with R^2 value of 0.9844. This shows that the drug release from PLHNCs is matrix diffusion controlled release process. The comparison of all the model has been given in Table 5-23.

Table 5-23 Regression coefficient value for all in-vitro release model of Docetaxel

Model	Regression coefficient
Higuchi model	0.9844
Korsmeyer peppas model	0.9816
First Order	0.8664
Hixon crowell model	0.7280
Zero order	0.7240

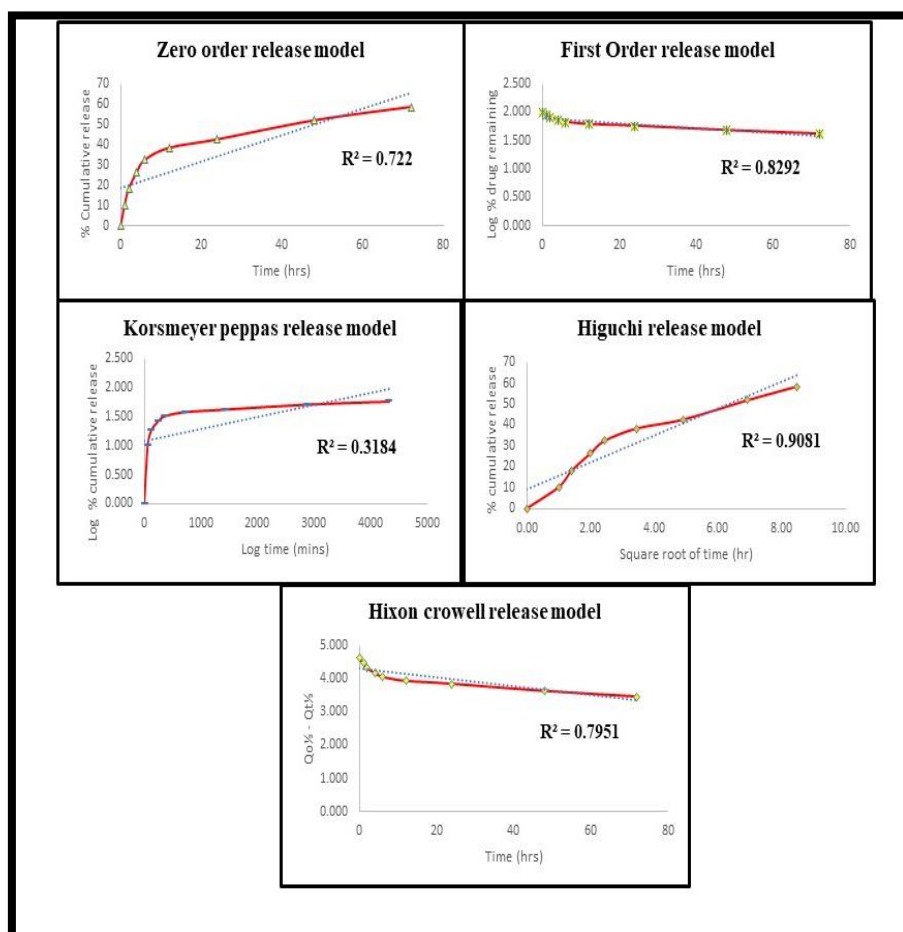


Figure 5-29 In-Vitro Release model of shRNA pDNA

From the kinetic model fitting analysis, it was concluded that for Docetaxel and shRNA loaded PLHNCs the best fit was Higuchi model (As shown in Figure 5-29) with R^2 value of

0.9081. This shows that the pDNA release from PLHNCs is diffusion controlled release process. The comparison of all the model has been given in Table 5-24.

Table 5-24 Regression coefficient value for all in-vitro release model of shRNA pDNA

Model	Regression coefficient
Higuchi model	0.9081
Korsmeyer peppas model	0.3184
First Order	0.8292
Hixon crowell model	0.7951
Zero order	0.722

5.7.7 Estimation of residual solvent by HS-Gas Chromatography

As per the ICH guidelines Q3C (R6) acetonitrile is CLASS II solvent and the permitted daily exposure limit is 4.1 mg/day which is equivalent to 410 ppm per day exposure (14). As shown in Figure 5-30, it was clearly noticed that concentration of acetonitrile in PLHNCs was reduced to a great extent during the stirring process hence stirring is required during the preparation of the PLHNCs.

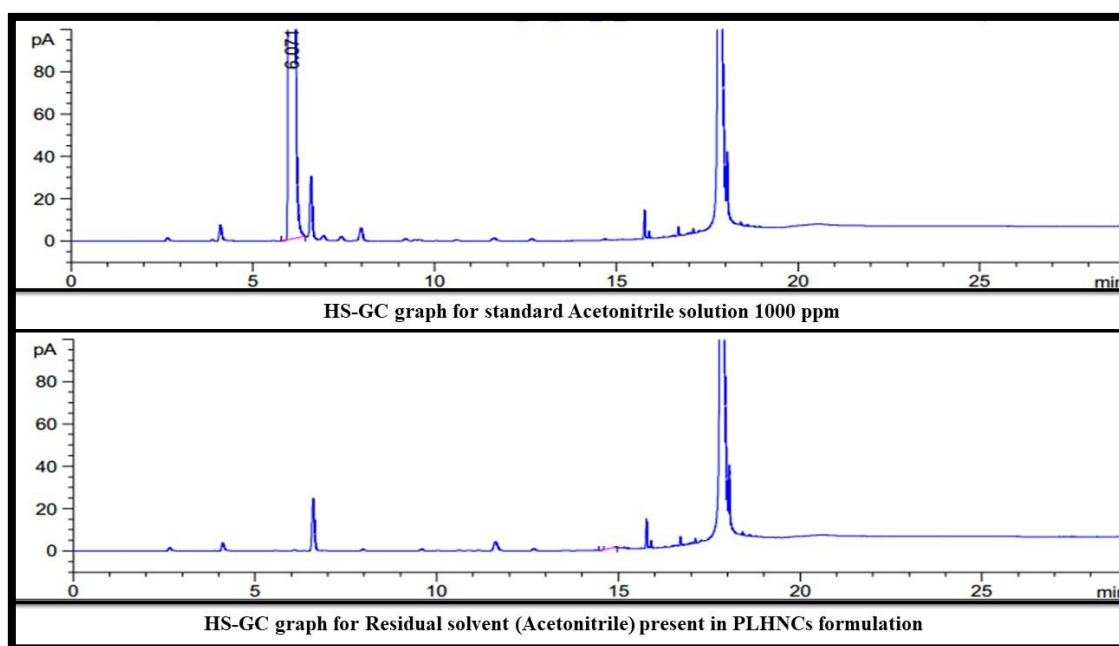


Figure 5-30 Graph of residual solvent (acetonitrile) estimation

As shown in Table 5-25 it was confirmed that acetonitrile present in the final optimized batch of PLHNC2 and PLHNC1 was within the daily limits of exposure as per ICH guidelines for residual solvents.

Table 5-25 Residual solvent (acetonitrile) analysis

Sr No.	Standard acetonitrile (ppm)	Acetonitrile in PLHNC1 (ppm)	Acetonitrile in PLHNC2 (ppm)
1	1000	67.8	72.65

5.7.8 Atomic Force Microscopy

Uniform and spherical shaped discrete particles of PLHNCs were seen in the morphological studies carried out by AFM. The particles with an average size of 150 nm were observed without any aggregation. The height histogram displays a reasonably narrow range of peak height corresponding to the thickness of the lipid bilayer and PEGylation layer from 20 to 35 nm. It was found that the average roughness (Ra) was 10.2 nm. These values showed a surface that was marginally rougher that may be attributed to the presence of the PEGylation sheet. The rise in roughness may be attributed to the presence of the PEGylation layer of DSPE-PEG-2000 in PLHNCs, which is important for stabilization and higher circulation time in in-vivo.

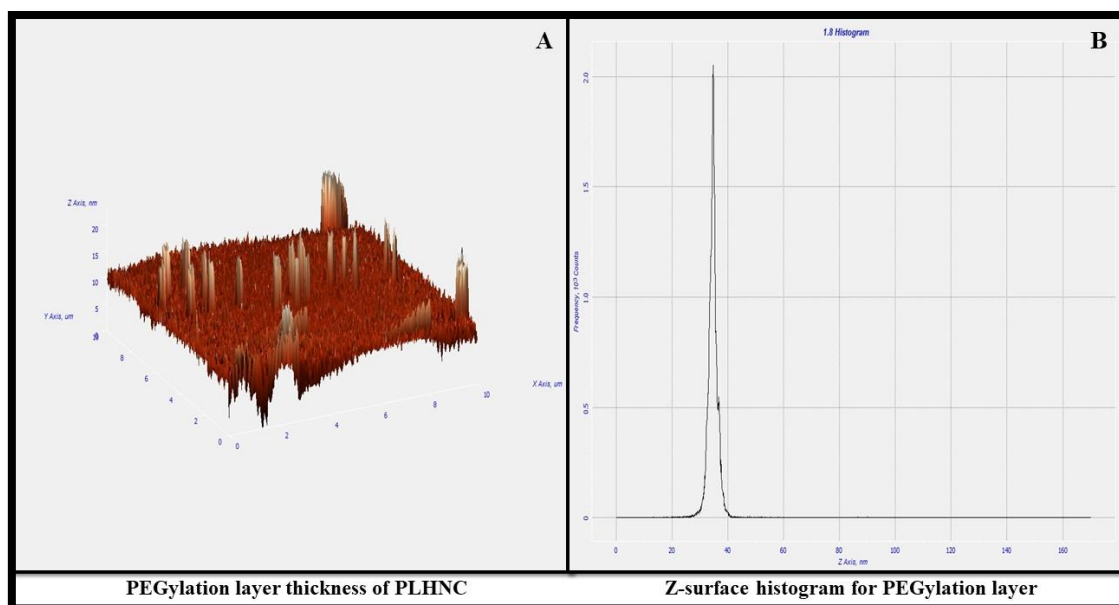


Figure 5-31 A) 3D image of PLHNC surface B) Z-surface histogram for estimation of PEGylation layer

5.8 REFERENCES

1. Mishra DK, Shandilya R, Mishra PK. Lipid based nanocarriers: a translational perspective. *Nanomedicine: Nanotechnology, Biology and Medicine*. 2018;14(7):2023-50.
2. Fang RH, Aryal S, Hu C-MJ, Zhang L. Quick synthesis of lipid– polymer hybrid nanoparticles with low polydispersity using a single-step sonication method. *Langmuir*. 2010;26(22):16958-62.
3. Veldhuizen EJ, Haagsman HP. Role of pulmonary surfactant components in surface film formation and dynamics. *Biochimica et Biophysica Acta (BBA)-Biomembranes*. 2000;1467(2):255-70.
4. Wu H, Khan MA, Hussain AS. Process control perspective for process analytical technology: integration of chemical engineering practice into semiconductor and pharmaceutical industries. *Chemical Engineering Communications*. 2007;194(6):760-79.
5. Lawrence XY. Pharmaceutical quality by design: product and process development, understanding, and control. *Pharmaceutical research*. 2008;25(4):781-91.
6. Singh B, Ahuja N. *Pharmaceutical Experimental Design (Drugs and the Pharmaceutical Sciences, Vol. 92)*, Edited by GA Lewis, D. Mathieu and R. Phan-Tan-Luu, Marcel Dekker, New York, 1999. vi+ 498 pp., 23.5 x15. 5 cm., 1.9 lb., Hardcover, ISBN 0-8247-9860-0, Price \$175.00. *International journal of pharmaceutics*. 2000;1(195):247-8.
7. Ferreira SC, Bruns R, Ferreira H, Matos G, David J, Brandao G, et al. Box-Behnken design: an alternative for the optimization of analytical methods. *Analytica chimica acta*. 2007;597(2):179-86.
8. Cohen H, Levy R, Gao J, Fishbein I, Kousaev V, Sosnowski S, et al. Sustained delivery and expression of DNA encapsulated in polymeric nanoparticles. *Gene therapy*. 2000;7(22):1896-905.
9. Patel J, Amrutiya J, Bhatt P, Javia A, Jain M, Misra A. Targeted delivery of monoclonal antibody conjugated docetaxel loaded PLGA nanoparticles into EGFR overexpressed lung tumour cells. *Journal of microencapsulation*. 2018;35(2):204-17.
10. Thanki K, van Eetvelde D, Geyer A, Fraire J, Hendrix R, Van Eygen H, et al. Mechanistic profiling of the release kinetics of siRNA from lipidoid-polymer hybrid nanoparticles in vitro and in vivo after pulmonary administration. *Journal of Controlled Release*. 2019;310:82-93.
11. Muthappa R, Purushothaman BK, Begum KMS, Maheswari PU. Kinetic Modeling and Optimization of the Release Mechanism of Curcumin from Folate Conjugated Hybrid BSA Nanocarrier. *Chemical Product and Process Modeling*. 2020;15(1).
12. Countryman S. Understanding the revisions to USP monograph< 467>: Residual solvents. *LC GC NORTH AMERICA*. 2007;25(6):60.
13. Gao W, Chan JM, Farokhzad OC. pH-responsive nanoparticles for drug delivery. *Molecular pharmaceutics*. 2010;7(6):1913-20.
14. Guideline IH. Q3C (R6).